

DESIGN AND OPTIMIZATION OF LANTHANIDE OXIDES BASED
CATALYSTS FOR CARBON DIOXIDE METHANATION

SALMIAH JAMAL BINTI MAT ROSID

UNIVERSITI TEKNOLOGI MALAYSIA

DESIGN AND OPTIMIZATION OF LANTHANIDE OXIDES BASED
CATALYSTS FOR CARBON DIOXIDE METHANATION

SALMIAH JAMAL BINTI MAT ROSID

A thesis submitted in fulfilment of the
requirements for the award of the degree of
Doctor of Philosophy (Chemistry)

Faculty of Science
Universiti Teknologi Malaysia

JULY 2015

For my beloved supervisor and family, who offered me unconditional love and a lot of support throughout the course of this report, my wonderful brothers and sister, and all my dearest friends who are always with me when I need them. Thanks for the support you all have given until now. May Allah bless you always.

ACKNOWLEDGEMENTS

Although I am indeed the sole author of this report, I am by no means the sole contributor. So many people have contributed to my report and it is now my great pleasure to take this opportunity to thank them.

Firstly, All Praise and Gratitude to Allah Almighty for without His benevolence and grace, I will not even be living right now to complete this project. I would like to take this opportunity to express my solemn thanks and utmost gratitude to my supervisors Prof. Dr. Wan Azelee Wan Abu Bakar and Assoc. Prof. Dr. Rusmidah Ali for guiding me throughout the course of this project. Their advice, suggestions and insight has helped me from the initial phase of this project to its completion, for which I am eternally grateful.

I also would like to say thanks to all lecturers and staff from the Department of Chemistry, and my fellow friends that had directly and indirectly helped me throughout this research project. I am grateful to Universiti Teknologi Malaysia (UTM) for providing the necessary facilities in presentation of this work, and Ministry of Science, Technology and Innovation (MOSTI) for offering me My Brain 15 (My PhD) and financial support in laboratory works.

Finally and most importantly, I am forever indebted to my parents and my siblings for their understanding, endless patience and encouragement when it most required. It is such a heart-warming experience I had, and such experience will always be with me.

ABSTRACT

The Malaysian crude natural gas contains toxic and acidic gases such as carbon dioxide, CO₂ (20-30%), and hydrogen sulfide, H₂S (0-1%), therefore it should be treated. The current gases treatment process including chemical solvents, adsorption process using hybrid solvents and membrane failed to meet the processing requirement. Instead, catalysts used for the CO₂ methanation have been extensively studied and high potential towards converting CO₂ gas to methane. In this research, a series of lanthanide oxide based catalysts supported on alumina and doped with manganese and ruthenium were prepared by wetness impregnation method. The lower performance of monometallic and bimetallic oxide catalysts have steered the exploration of trimetallic oxide catalyst. The potential trimetallic oxide catalysts were calcined at 400°C, 700°C, and 1000°C for 5 hours separately. In-home-built micro reactor, Fourier transform infrared (FTIR) spectroscopy and gas chromatography analysis (GC) were used to study the catalytic performance by determining the percentage of CO₂ conversion and also the percentage of CH₄ formation. From the catalytic screening, it was found that the catalysts with Ru/Mn/Ce (5:35:60)/Al₂O₃ calcined at 700°C, and Ru/Mn/Sm (5:35:60)/Al₂O₃ calcined at 1000°C achieved 100% CO₂ conversion, Ru/Mn/Pr (5:30:65)/Al₂O₃ calcined at 800°C achieved 96% CO₂ conversion were potential catalysts. The active species in the methanation reaction for each catalyst were MnO₂, and RuO₂ and CeO₂ or Sm₂O₃ or Pr₂O₃ respectively. Using two series furnace reactors, all three potential catalysts showed the increasing of CH₄ formation. For optimization, the parameters studied were calcination temperatures, based loadings, and catalyst dosage. The optimization was done by using response surface methodology (RSM) with Box-Behnken design which showed the significant parameters and optimum result of cerium with calcination temperature of 697.47°C, based metal ratio of 60.38% and catalyst dosage 6.94 g as suggested by RSM. This result was tested and verified experimentally with difference of only 1%. X-rays diffraction analysis showed that the catalysts imposed an amorphous phase, while field emission scanning electron microscopy illustrated the catalyst surface was covered with small and dispersed particles with undefined shape. From electron dispersive X-rays analysis revealed that there were a reduction of Ru in the used catalyst compared to the fresh catalyst for each potential catalysts. Nitrogen gas adsorption showed that the catalysts were mesoporous structure with type H3 hysteresis loop and Type IV isotherm. Electron spin resonance spectrum showed a free electron interaction due to the presence of the peak for each potential catalyst. Temperature programmed reduction analysis of Ru/Mn/Ce (5:35:60)/Al₂O₃ catalyst showed more reducible species compared to catalysts containing Sm and Pr due to the presences of more reduce species at lower reduction temperature. The postulated methanation reaction follows the Langmuir Hinselwood mechanism which initially involves adsorption of CO₂ and H₂ gases on the catalyst surface. For Ru/Mn/Ce (5:35:60)/Al₂O₃ and Ru/Mn/Sm (5:35:60)/Al₂O₃ catalysts the product obtained were CH₄, CH₃OH and H₂O. Meanwhile, for Ru/Mn/Pr (5:30:65)/Al₂O₃ catalyst only CH₄ and H₂O were observed as a products of the reaction. Lastly, the spent catalysts were successfully regenerated by running under O₂ flow at 100°C for 1 hour.

ABSTRAK

Gas asli mentah Malaysia mengandungi gas toksik dan berasid seperti dioksida, CO₂ (20-30%), dan hidrogen sulfida, H₂S (0-1%). Oleh itu, ia perlu dirawat. Pada masa kini, proses rawatan gas termasuk pelarut kimia, proses penjerapan menggunakan pelarut hibrid dan membran gagal memenuhi keperluan pemprosesan. Sebaliknya, mangkin yang digunakan untuk metanasi CO₂ telah dikaji secara meluas dan mempunyai potensi yang tinggi untuk menukarkan gas CO₂ kepada metana. Dalam kajian ini, satu siri mangkin berasaskan lantanida oksida disokong pada alumina dan didopkan dengan mangan dan rutenium telah disediakan dengan kaedah pengisitepuan basah. Prestasi mangkin mono logam dan dwilogam oksida yang lebih rendah telah mendorong kepada penerokaan mangkin trilogram oksida. Mangkin trilogram oksida yang berpotensi telah dikalsin pada suhu 400°C, 700°C, dan 1000°C selama 5 jam secara berasingan. Reaktor mikro buatan tempatan dengan spektroskopi infra-merah transformasi Fourier (FTIR) dan gas kromatografi (GC) telah digunakan untuk mengkaji prestasi mangkin dengan menentukan peratusan penukaran CO₂ dan juga peratusan pembentukan CH₄. Daripada penyaringan mangkin didapati bahawa mangkin Ru/Mn/Ce (5:35:60)/Al₂O₃ pada suhu 700°C, dan Ru/Mn/Sm (5:35:60)/Al₂O₃ pada suhu 1000°C mencapai 100% penukaran CO₂, Ru/Mn/Pr (5:30:65)/Al₂O₃ pada suhu 800°C mencapai 96% penukaran CO₂ adalah mangkin-mangkin berpotensi. Dalam tindak balas metanasi, spesies aktif untuk setiap mangkin adalah MnO₂ dan RuO₂ dan CeO₂ atau Sm₂O₃ atau Pr₂O₃. Dengan menggunakan reaktor relau dua siri, ketiga-tiga mangkin berpotensi menunjukkan peningkatan pembentukan CH₄. Untuk pengoptimuman, parameter yang dikaji ialah suhu pengkalsinan, nisbah asas, dan dos pemangkin. Proses pengoptimum ini telah dilakukan dengan menggunakan kaedah respon permukaan (RSM) dengan reka bentuk Box-Behnken yang menunjukkan parameter penting dan keputusan yang optimum untuk cerium dengan suhu pengkalsinan 697.47°C, nisbah asas 60.38% dan dos pemangkin 6.94 g seperti yang dicadangkan oleh RSM. Keputusan ini telah diuji dan disahkan secara eksperimen dengan perbezaan hanya 1%. Analisis belauan sinar X menunjukkan bahawa mangkin membentuk fasa amorfus, manakala pelepasan medan mikroskopi pengimbasan elektron menggambarkan permukaan mangkin itu dipenuhi dengan zarah kecil dan tersebar dengan bentuk yang tidak sekata. Dari tenaga serakan sinar-X analisis pula menunjukkan terdapat pengurangan Ru pada mangkin yang telah digunakan berbanding dengan mangkin yang belum digunakan bagi setiap mangkin berpotensi. Penjerapan gas nitrogen menunjukkan mangkin berstruktur liang meso dengan keluk jenis histerisis H3 dan isoterma Jenis IV. Spektrum resonan putaran elektron menunjukkan interaksi elektron bebas yang disebabkan oleh kehadiran puncak bagi setiap mangkin berpotensi. Analisis penyahjerapan pengaturcaraan suhu dari mangkin Ru/Mn/Ce (5:35:60)/Al₂O₃ menunjukkan banyak spesies terturun berbanding mangkin yang mengandungi Sm dan Pr kerana kehadiran banyak spesies terturun pada suhu yang lebih rendah. Tindak balas metanasi diramal mengikut mekanisme Langmuir Hinselwood yang pada mulanya melibatkan penjerapan gas CO₂ dan H₂ pada permukaan mangkin. Untuk mangkin Ru/Mn/Ce (5:35:60)/Al₂O₃ dan Ru/Mn/Sm (5:35:60)/Al₂O₃, produk yang dapat adalah CH₄, CH₃OH, dan H₂O. Manakala, untuk mangkin Ru/Mn/Pr (5:30:65)/Al₂O₃ hanya CH₄ dan H₂O dihasilkan sebagai produk tindak balas. Akhir sekali, pemangkin yang telah digunakan dan tidak aktif dijana semula di bawah keadaan aliran O₂ pada 100°C selama 1 jam.

TABLE OF CONTENTS

CHAPTER	TITLE	PAGE
	DECLARATION	ii
	DEDICATION	iii
	ACKNOWLEDGEMENT	iv
	ABSTRACT	v
	ABSTRAK	vi
	TABLE OF CONTENTS	vii
	LIST OF TABLES	xvii
	LIST OF FIGURES	xxiii
	LIST OF ABBREVIATIONS	xxxiii
	LIST OF APPENDICES	xxxv
1	INTRODUCTION	1
	1.1 Background of study	1
	1.2 Gas Purification Process	5
	1.3 Catalytic Methanation	7
	1.4 Response Surface Methodology	8
	1.5 Mechanism of Methanation Reaction Process	10
	1.6 Statement of Problem	11
	1.7 Objectives	13
	1.8 Significance of Study	13
	1.9 Scope of Study	14
2	LITERATURE REVIEW	15
	2.1 Introduction	15
	2.2 Methanation Catalysts	16

2.2.1	Lanthanide Catalyst Over Methanation Reaction	17
2.2.2	Transition Metal Influence Over Methanation Reaction	22
2.2.3	Noble Metals Over Methanation Reaction	24
2.2.4	Supports over Methanation Reaction	26
2.3	Response Surface Methodology	28
2.4	Mechanistic Studies	30
3	EXPERIMENTAL	36
3.1	Frame of Work	36
3.2	General Apparatus	36
3.3	Chemicals and Reagents	37
3.4	Catalyst Preparation	38
3.4.1	Incipient Wetness Impregnation Method	38
3.5	Catalytic Activity Measurement	39
3.5.1	Catalytic Screening by Fourier Transform Infrared (FTIR)	40
3.5.2	Methane Measurement Via Gas Chromatography	41
3.5.3	High Performance Liquid Chromatography (HPLC) Analysis	43
3.6	Optimization parameters	43
3.6.1	Optimization of The Based Loading	43
3.6.2	Calcination Temperature of Supported Catalysts	44
3.6.3	Optimization of The Ruthenium Loading	44
3.6.4	Catalyst Dosages	44
3.6.5	Double Series of Micro-Recto	45
3.7	Statistical Analysis	45
3.7.1	Test For Significance of The Regression Model	45

3.7.2	Test For Significance On Individual Model Coefficients	45
3.7.3	Test For Lack of Fit	46
3.8	Mechanistic Study	47
3.9	Reproducibility Testing	47
3.10	Regeneration Activity	47
3.11	Stability Testing	48
3.12	Characterization	48
3.12.1	X-Ray Diffraction Spectroscopy (XRD)	48
3.12.2	Field Emission Scanning Electron Microscopy- Energy Dispersive X-Ray (FESEM-EDX)	49
3.12.3	Nitrogen Adsorption Analysis (NA)	49
3.12.4	Fourier Transform Infrared Spectroscopy (FTIR)	50
3.12.5	Thermogravimetry Analysis Differential Thermal Analysis (TGA-DTA)	50
3.12.6	X-Ray Photoelectron Spectroscopy (XPS)	50
3.12.7	Temperature Programmed Reduction (TPR)	51
3.12.8	Temperature Programmed Desorption (TPD)	51
3.12.9	Electron Spin Resonance (ESR)	52
4	SCREENING OF LANTHANIDE BASED OXIDE CATALYST	53
4.1	Catalytic Activity Measurement Using FTIR Analysis	53
4.2	Catalytic Activity Screening On Alumina Supported Lanthanide Oxide Based Catalyst For CO ₂ Methanation Reaction	54

4.3	Catalytic Activity Screening of Alumina Supported Lanthanide Oxide Based Catalyst With One Dopant For CO ₂ /H ₂ Methanation Reaction	55
4.4	Catalytic Activity Screening of Alumina Supported Lanthanide Oxide Based Catalyst With Co-Dopants For CO ₂ /H ₂ Methanation Reaction	62
4.4.1	Catalytic Activity Screening of Trimetallic Oxide Catalyst Calcined At 400°C For 5 Hours	62
4.4.2	Catalytic Activity Screening of Trimetallic Oxide Catalyst Calcined At 700°C and 1000°C For 5 Hours	66
4.5	Determination of CO ₂ /H ₂ Methanation Reaction by Gas Chromatography	71
5	OPTIMIZATION, CHARACTERIZATION, AND MECHANISTIC STUDY OF CERIUM CATALYST	74
5.1	Characterization of Catalysts	74
5.1.1	X-Ray Diffraction Analysis (XRD) For Ru/Mn/Ce (5:35:60)/Al ₂ O ₃ Catalyst	74
5.1.2	X-Ray Photoelectron Spectroscopy (XPS) For Ru/Mn/Ce (5:35:60)/Al ₂ O ₃ Catalyst	81
5.1.3	Electron Spin Resonance (ESR) For Ru/Mn/Ce (5:35:60)/Al ₂ O ₃ Catalyst	87
5.1.4	Temperature Programmed Reduction (TPR) For Ru/Mn/Ce (5:35:60)/Al ₂ O ₃ Catalyst	88
5.1.5	Temperature Programmed Desorption (TPD) For Ru/Mn/Ce (5:35:60)/Al ₂ O ₃ Catalyst	91
5.1.6	Field Emission Scanning Electron Microscopy (FESEM) For Ru/Mn/Ce (5:35:60)/Al ₂ O ₃ Catalyst	93

5.1.7	Electron-Dispersive X-Rays (EDX) For Ru/Mn/Ce (5:35:60)/Al ₂ O ₃ Catalyst	95
5.1.8	Nitrogen Adsorption Analysis (NA) for Ru/Mn/Ce (5:35:60)/Al ₂ O ₃ Catalyst	98
5.1.9	Thermogravimetry Analysis (TGA-DTA) for Ru/Mn/Ce (5:35:60)/Al ₂ O ₃ Catalyst	102
5.1.10	Fourier Transform Infrared Spectroscopy (FTIR) for Ru/Mn/Ce (5:35:60)/Al ₂ O ₃ Catalyst	104
5.2	Catalytic Activity of The Potential Ru/Mn/Ce (5:35:60)/Al ₂ O ₃ Catalyst	105
5.2.1	Effect of Calcination Temperature	105
5.2.2	Effect of Various Metal Oxide Based Loading	108
5.2.3	Effect of Catalyst Loading	110
5.2.4	Effect of Various Ruthenium Loading	111
5.3	Catalyst Testing On CO ₂ Methanation Reaction Using Double Reactors	112
5.4	Detection of Methane By Gas Chromatography For CO ₂ Methanation Reaction for Ru/Mn/Ce (5:35:60)/Al ₂ O ₃ Catalyst	114
5.5	Detection of Methanol By High Performance Liquid Chromatography (HPLC) for CO ₂ Methanation Reaction for Ru/Mn/Ce (5:35:60)/Al ₂ O ₃ Catalyst	115
5.6	Reproducibility Test for CO ₂ Methanation Reaction for Ru/Mn/Ce (5:35:60)/Al ₂ O ₃ Catalyst	117
5.7	Stability Testing for CO ₂ Methanation Reaction for Ru/Mn/Ce (5:35:60)/Al ₂ O ₃ Catalyst	118
5.8	Regeneration Test for CO ₂ Methanation Reaction for Ru/Mn/Ce (5:35:60)/Al ₂ O ₃ Catalyst	119
5.9	Response Surface Methodology	120
5.9.1	Box-Behnken Design (BBD)	120

5.9.1.1	Optimization of Cerium Catalyst Preparation Condition	121
5.9.1.2	Regression Model and ANOVA Analysis	122
5.9.1.3	Effect of Parameters With Response Surface and Contour Plotting	124
5.9.1.4	Optimization Response and Confirmation Test	129
6	OPTIMIZATION, CHARACTERIZATION, AND MECHANISTIC STUDY OF SAMARIUM CATALYST	131
6.1	Characterization of Catalysts	131
6.1.1	X-Ray Diffraction Analysis (XRD) For Ru/Mn/Sm (5:35:60)/Al ₂ O ₃ Catalyst	131
6.1.2	X-Ray Photoelectron Spectroscopy (XPS) For Ru/Mn/Sm (5:35:60)/Al ₂ O ₃ Catalyst	137
6.1.3	Electron Spin Resonance (ESR) For Ru/Mn/Sm (5:35:60)/Al ₂ O ₃ Catalyst	144
6.1.4	Temperature Programmed Reduction (TPR) For Ru/Mn/Sm (5:35:60)/Al ₂ O ₃ Catalyst	146
6.1.5	Temperature Programmed Desorption (TPD) For Ru/Mn/Sm (5:35:60)/Al ₂ O ₃ Catalyst	148
6.1.6	Field Emission Scanning Electron Microscopy (FESEM) For Ru/Mn/Sm (5:35:60)/Al ₂ O ₃ Catalyst	150
6.1.7	Electron-Dispersive X-Rays (EDX) For Ru/Mn/Sm (5:35:60)/Al ₂ O ₃ Catalyst	152
6.1.8	Nitrogen Adsorption Analysis (NA) For Ru/Mn/Sm (5:35:60)/Al ₂ O ₃ Catalyst	156

6.1.9	Thermogravimetry Analysis (TGA-DTA) For Ru/Mn/Sm (5:35:60)/Al ₂ O ₃ Catalyst	158
6.1.10	Fourier Transform Infrared Spectroscopy (FTIR) For Ru/Mn/Sm (5:35:60)/Al ₂ O ₃ Catalyst	160
6.2	Catalytic Activity of The Potential Ru/Mn/Sm (5:35:60)/Al ₂ O ₃ Catalyst	162
6.2.1	Effect of Calcination Temperature	162
6.2.2	Effect of Various Metal Oxide Based Loading	164
6.2.3	Effect of Catalyst Loading	166
6.2.4	Effect of Various Ruthenium Loading	167
6.3	Catalyst Testing On CO ₂ Methanation Reaction Using Double Reactors	167
6.4	Detection of Methane By Gas Chromatography for CO ₂ Methanation Reaction for Ru/Mn/Sm (5:35:60)/Al ₂ O ₃ Catalyst	170
6.5	Detection of Methanol By High Performance Liquid Chromatography (HPLC) for CO ₂ Methanation Reaction for Ru/Mn/Sm (5:35:60)/Al ₂ O ₃ Catalyst	172
6.6	Reproducibility Test for CO ₂ Methanation Reaction for Ru/Mn/Sm (5:35:60)/Al ₂ O ₃ Catalyst	173
6.7	Stability Testing for CO ₂ Methanation Reaction for Ru/Mn/Sm (5:35:60)/Al ₂ O ₃ Catalyst	175
6.8	Regeneration Test for CO ₂ Methanation Reaction for Ru/Mn/Sm (5:35:60)/Al ₂ O ₃ Catalyst	176
6.9	Response Surface Methodology	177
6.9.1	Box-Behnken Design (BBD)	177
6.9.1.1	Optimization of Samarium Catalyst Preparation Condition	178
6.9.1.2	Regression Model and ANOVA Analysis	179

6.9.1.3	Effect of Parameters With Response Surface and Contour Plotting	180
6.9.1.4	Optimization Response and Confirmation	185
7	OPTIMIZATION, AND CHARACTERIZATION, OF PRASEODYNIUM CATALYST	187
7.1	Characterization of Catalysts	187
7.1.1	X-Ray Diffraction Analysis (XRD) for Ru/Mn/Pr (5:30:65)/Al ₂ O ₃ Catalyst	187
7.1.2	X-Ray Photoelectron Spectroscopy (XPS) for Ru/Mn/Pr (5:30:65)/Al ₂ O ₃ Catalyst	192
7.1.3	Electron Spin Resonance (ESR) for Ru/Mn/Pr (5:30:65)/Al ₂ O ₃ Catalyst	197
7.1.4	Temperature Programmed Reduction (TPR) for Ru/Mn/Pr (5:30:65)/Al ₂ O ₃ Catalyst	198
7.1.5	Temperature Programmed Desorption (TPD) for Ru/Mn/Pr (5:30:65)/Al ₂ O ₃ Catalyst	201
7.1.6	Field Emission Scanning Electron Microscopy (FESEM) for Ru/Mn/Pr (5:30:65)/Al ₂ O ₃ Catalyst	202
7.1.7	Electron-Dispersive X-Rays (EDX) for Ru/Mn/Pr (5:30:65)/Al ₂ O ₃ Catalyst	204
7.1.8	Nitrogen Adsorption Analysis (NA) for Ru/Mn/Pr (5:30:65)/Al ₂ O ₃ Catalyst	208
7.1.9	Thermogravimetry Analysis (TGA-DTA) for Ru/Mn/Pr (5:30:65)/Al ₂ O ₃ Catalyst	211
7.1.10	Fourier Transform Infrared Spectroscopy (FTIR) for Ru/Mn/Pr (5:30:65)/Al ₂ O ₃ Catalyst	213

7.2	Catalytic Activity of The Potential Ru/Mn/Pr (5:30:65)/Al ₂ O ₃ Catalyst	214
7.2.1	Effect of Calcination Temperature	215
7.2.2	Effect of Various Metal Oxide Based Loading	217
7.2.3	Effect of Catalyst Loading	218
7.2.4	Effect of Various Ruthenium Loading	220
7.3	Catalyst Testing On CO ₂ Methanation Reaction Using Double Reactors	221
7.4	Detection of Methane By Gas Chromatography for CO ₂ Methanation Reaction for Ru/Mn/Pr (5:30:65)/Al ₂ O ₃ Catalyst	222
7.5	Reproducibility Test for CO ₂ Methanation Reaction for Ru/Mn/Pr (5:30:65)/Al ₂ O ₃ Catalyst	224
7.6	Stability Testing for CO ₂ Methanation Reaction for Ru/Mn/Pr (5:30:65)/Al ₂ O ₃ Catalyst	225
7.7	Regeneration Test for CO ₂ Methanation Reaction for Ru/Mn/Pr (5:30:65)/Al ₂ O ₃ Catalyst	226
7.8	Response Surface Methodology	227
7.8.1	Box-Behnken Design (BBD)	228
7.8.1.1	Optimization of Praseodymium Catalyst Preparation Condition	228
7.8.1.2	Regression Model and ANOVA Analysis	229
7.8.1.3	Effect of Parameters With Response Surface and Contour Plotting	231
7.8.1.4	Optimization Response and Confirmation	235
8	MECHANISTIC STUDY	237
8.1	Summarization of Potential Catalysts	237
8.2	Mechanism of Methanation Reaction	237

8.3.	Products Analysis by Ru/Mn/Ce (5:35:60)/Al ₂ O ₃ and Ru/Mn/Sm (5:35:60)/Al ₂ O ₃ catalysts during methanation reaction	238
8.3.2	Mechanism of Methanation Reaction by Ru/Mn/Ce (5:35:60)/ Al ₂ O ₃ and Ru/Mn/Sm (5:35:60)/Al ₂ O ₃	241
8.4.	Products Analysis by Ru/Mn/Pr (5:30:65)/ Al ₂ O ₃ catalyst during methanation reaction	244
8.4.2	Mechanism of Methanation Reaction by Ru/Mn/Pr (5:30:65)/ Al ₂ O ₃	245
9	CONCLUSION AND RECOMMENDATIONS	248
9.1	Conclusion	248
9.2	Recommendations	250
	REFERENCES	251
	Appendices A-H	272-280

LIST OF TABLES

TABLE NO.	TITLE	PAGE
1.1	Chemical composition of Malaysian natural gas	2
3.1	Wavenumber of CO ₂ , CO, CH ₄ and OH in FTIR spectrum	40
4.1	Percentage conversion of CO ₂ catalyzed by lanthanum oxide based catalysts with dopant (Mn or Co) and co-dopant (Ru) after calcined at 400°C for CO ₂ /H ₂ methanation reaction	62
4.2	Percentage conversion of CO ₂ catalyzed by cerium oxide based catalysts with dopant (Mn or Co) and co-dopant (Ru) after calcined at 400°C for CO ₂ /H ₂ methanation reaction	62
4.3	Percentage conversion of CO ₂ catalyzed by samarium oxide based catalysts with dopant (Mn or Co) and co-dopant (Ru) after calcined at 400°C for CO ₂ /H ₂ methanation reaction	63
4.4	Percentage conversion of CO ₂ catalyzed by praseodymium oxide based catalysts with dopant (Mn or Co) and co-dopant (Ru) after calcined at 400°C for CO ₂ /H ₂ methanation reaction	63
4.5	Percentage conversion of CO ₂ catalyzed by neodymium oxide based catalysts with dopant (Mn or Co) and co-dopant (Ru) after calcined at 400°C for CO ₂ /H ₂ methanation reaction	64
4.6	Percentage conversion of CO ₂ catalyzed by gadolinium oxide based catalysts with dopant (Mn or Co) and co-dopant (Ru) after calcined at 400°C for CO ₂ /H ₂ methanation reaction	64

4.7	Percentage conversion of CO ₂ catalyzed by lanthanum oxide based catalysts with dopant (Mn or Co) and co-dopant (Ru) after calcined at 400°C, 700°C, and 1000°C for CO ₂ /H ₂ methanation reaction	66
4.8	Percentage conversion of CO ₂ catalyzed by cerium oxide based catalysts with dopant (Mn or Co) and co-dopant (Ru) after calcined at 400°C, 700°C, and 1000°C for CO ₂ /H ₂ methanation reaction	67
4.9	Percentage conversion of CO ₂ catalyzed by samarium oxide based catalysts with dopant (Mn or Co) and co-dopant (Ru) after calcined at 400°C, 700°C, and 1000°C for CO ₂ /H ₂ methanation reaction	68
4.10	Percentage conversion of CO ₂ catalyzed by praseodymium oxide based catalysts with dopant (Mn or Co) and co-dopant (Ru) after calcined at 400°C, 700°C, and 1000°C for CO ₂ /H ₂ methanation reaction	68
4.11	Percentage conversion of CO ₂ catalyzed by neodymium oxide based catalysts with dopant (Mn or Co) and co-dopant (Ru) after calcined at 400°C, 700°C, and 1000°C for CO ₂ /H ₂ methanation reaction	69
4.12	Percentage conversion of CO ₂ catalyzed by gadolinium oxide based catalysts with dopant (Mn or Co) and co-dopant (Ru) after calcined at 400°C, 700°C, and 1000°C for CO ₂ /H ₂ methanation reaction	70
4.13	Testing results of in-situ reactions of methane formation over various alumina supported catalysts at 1000°C calcination temperature	72
5.1	Peaks assignment in XRD pattern of Ru/Mn/Ce (5:35:60)/Al ₂ O ₃ catalyst calcined at 600°C, 700°C, 800°C, and 1000°C for 5 hours	76
5.2	Peaks assignment in XRD pattern of Ru/Mn/Ce (5:35:60)/Al ₂ O ₃ catalyst calcined at 1000°C for 5 hours with different Ce loadings	79

5.3	Parameters obtained by deconvolution of XPS spectra for Ce (<i>3d</i>) peaks in fresh Ru/Mn/Ce (5:35:60)/Al ₂ O ₃ catalyst	82
5.4	Parameters obtained by deconvolution of XPS spectra for O (<i>1s</i>) peaks in fresh Ru/Mn/Ce (5:35:60)/Al ₂ O ₃ catalyst	83
5.5	Parameters obtained by deconvolution of XPS spectra for Al (<i>2p</i>) peaks in fresh Ru/Mn/Ce (5:35:60)/Al ₂ O ₃ catalyst	84
5.6	Parameters obtained by deconvolution of XPS spectra for Mn (<i>2p</i>) peaks in fresh Ru/Mn/Ce (5:35:60)/Al ₂ O ₃ catalyst	85
5.7	Reduction amount of Ru/Mn/Ce (5:35:60)/Al ₂ O ₃ catalyst at different calcination temperature	90
5.8	The amount of CO ₂ adsorbed on Ru/Mn/Ce (5:35:60)/Al ₂ O ₃ catalyst calcined at 700°C calcination temperature	91
5.9	Elemental composition from EDX analysis for Ru/Mn/Ce (5:35:60)/Al ₂ O ₃ catalyst calcined at 400°C, 600°C, 700°C, 800°C and 1000°C for 5 hours	94
5.10	BET surface area, average pore diameter and pore volume of Ru/Mn/Ce (5:35:60)/Al ₂ O ₃ catalyst at different calcination temperature	98
5.11	Summary results of TGA analysis of Ru/Mn/Ce (5:35:60)/Al ₂ O ₃ catalyst	102
5.12	FTIR analysis for the calcined of Ru/Mn/Ce (5:35:60)/Al ₂ O ₃ catalyst at 600°C, 700°C, and 800°C for 5 hours	104
5.13	Percentage conversion of CO ₂ by Ru/Mn/Ce (5:35:60)/Al ₂ O ₃ calcined various calcination temperatures for 5 hours	106
5.14	Percentage conversion of CO ₂ by Ru/Mn/Ce (5:35:60)/Al ₂ O ₃ calcined at 700°C with various base loading for 5 hours	107
5.15	Percentage conversion of CO ₂ by Ru/Mn/Ce (5:35:60)/Al ₂ O ₃ calcined at 700°C with various catalyst loading	109
5.16	Percentage conversion of CO ₂ by various loadings of ruthenium for cerium oxide catalyst calcined at 700°C for 5 hours	110

5.17	Comparison of CO ₂ conversion for Ru/Mn/Ce(5:35:60)/Al ₂ O ₃ catalyst by using double reactors calcined at 700°C for 5 hours	111
5.18	Methane formation in in-situ methanation reactions over Ru/Mn/Ce (5:35:60)/Al ₂ O ₃ catalysts at various calcination temperature	114
5.19	Levels of the optimization conditions	119
5.20	Experimental design for CO ₂ conversion and results response for cerium catalyst	120
5.21	ANOVA data (partial sum of squares) for response surface model (response: CO ₂ conversion)	121
6.1	Peaks assignment in XRD pattern of Ru/Mn/Sm (5:35:60)/Al ₂ O ₃ catalyst calcined at 400°C, 700°C, 900°C, 1000°C and 1100°C for 5 hours	131
6.2	Peaks assignment in XRD pattern of Ru/Mn/Sm (5:35:60)/Al ₂ O ₃ catalyst with various based loadings calcined at 1000°C for 5 hours	134
6.3	Parameters obtained by deconvolution of XPS spectra for O (1s) peaks in fresh Ru/Mn/Sm (5:35:60)/Al ₂ O ₃ catalyst	137
6.4	Parameters obtained by deconvolution of XPS spectra for Al (2p) peaks in fresh Ru/Mn/Sm (5:35:60)/Al ₂ O ₃ catalyst	138
6.5	Parameters obtained by deconvolution of XPS spectra for Mn (2p) peaks in fresh Ru/Mn/Sm (5:35:60)/Al ₂ O ₃ catalyst	139
6.6	Parameters obtained by deconvolution of XPS spectra for Sm (3d) peaks in fresh Ru/Mn/Sm (5:35:60)/Al ₂ O ₃ catalyst	140
6.7	Parameters obtained by deconvolution of XPS spectra for Ru (3p) peaks in fresh Ru/Mn/Sm (5:35:60)/Al ₂ O ₃ catalyst	142
6.8	Reduction amount of Ru/Mn/Sm (5:35:60)/Al ₂ O ₃ catalyst at different calcination temperature	146
6.9	The amount of CO ₂ adsorbed on Ru/Mn/Sm(5:35:60)/Al ₂ O ₃ catalyst calcined at 1000°C calcination temperature	148

6.10	Elemental composition from EDX analysis for Ru/Mn/Sm (5:35:60)/Al ₂ O ₃ catalyst calcined at 400°C, 700°C, 900°C, 1000°C and 1100°C for 5 hours	150
6.11	BET surface area, average pore diameter and pore volume of Ru/Mn/Sm (5:35:60)/Al ₂ O ₃ catalyst at different calcination temperatures	154
6.12	Summary results of TGA analysis of Ru/Mn/Sm (5:35:60)/Al ₂ O ₃ catalyst	159
6.13	FTIR analysis data for the calcined of Ru/Mn/Sm (5:35:60)/ Al ₂ O ₃ catalyst at 900°C, 1000°C, and 1100°C for 5 hours	160
6.14	Percentage conversion of CO ₂ by Ru/Mn/Sm (5:35:60)/Al ₂ O ₃ calcined at various calcination temperatures for 5 hours	161
6.15	Percentage conversion of CO ₂ by Ru/Mn/Sm (5:35:60)/Al ₂ O ₃ calcined at 1000°C with various base loading	163
6.16	Percentage conversion of CO ₂ by Ru/Mn/Sm (5:35:60)/Al ₂ O ₃ calcined at 1000°C various catalyst loading	164
6.17	Percentage conversion of CO ₂ by various loadings of ruthenium for Ru/Mn/Sm (5:35:60)/ Al ₂ O ₃ catalyst at 1000°C	166
6.18	Comparison of CO ₂ conversion for Ru/Mn/Sm (5:35:60)/Al ₂ O ₃ catalyst calcined at 1000°C for 5 hours by using double reactor	167
6.19	Methane formation in in-situ methanation reactions over Ru/Mn/Sm (5:35:60)/Al ₂ O ₃ catalyst at various calcination temperatures	169
6.20	Levels of the optimization conditions for samarium catalyst	176
6.21	Experimental design for CO ₂ conversion and results response for samarium catalyst	176
6.22	ANOVA data (partial sum of squares) for response surface model (response: CO ₂ conversion)	177

7.1	Peaks assignment in XRD pattern of Ru/Mn/Pr (5:30:65)/Al ₂ O ₃ catalyst calcined at 400°C, 700°C, 800°C, 900°C and 1000°C for 5 hours	187
7.2	Peaks assignment in XRD pattern of Ru/Mn/Pr (5:30:65)/Al ₂ O ₃ catalyst calcined at 800°C for 5 hours with different Pr loadings	189
7.3	Parameters obtained by deconvolution of XPS spectrum for O (1s) peaks in fresh Ru/Mn/Pr (5:30:65)/Al ₂ O ₃ catalyst	191
7.4	Parameters obtained by deconvolution of XPS spectrum for Al (2p) peaks in fresh Ru/Mn/Pr (5:30:65)/Al ₂ O ₃ catalyst	192
7.5	Parameters obtained by deconvolution of XPS spectrum for Mn (2p) peaks in fresh Ru/Mn/Pr (5:30:65)/Al ₂ O ₃ catalyst	193
7.6	Parameters obtained by deconvolution of XPS spectrum for Pr (3d) peaks in fresh Ru/Mn/Pr (5:30:65)/Al ₂ O ₃ catalyst	195
7.7	Reduction amount of Ru/Mn/Pr (5:30:65)/Al ₂ O ₃ catalyst at different calcination temperatures	198
7.8	The amount of CO ₂ adsorbed on Ru/Mn/Pr (5:30:65)/Al ₂ O ₃ catalyst calcined at 800°C calcination temperature	200
7.9	Elemental composition from EDX analysis for Ru/Mn/Pr (5:30:65)/Al ₂ O ₃ catalyst calcined at 400°C, 700°C, 800°C, 900°C and 1000°C for 5 hours	202
7.10	BET surface area, average pore diameter and pore volume of Ru/Mn/Pr (5:30:65)/Al ₂ O ₃ catalyst at different calcination temperature	206
7.11	Summary results of TGA analysis of Ru/Mn/Pr (5:30:65)/Al ₂ O ₃ catalyst	210
7.12	FTIR analysis for the calcined of Ru/Mn/Pr (5:30:65)/Al ₂ O ₃ catalyst at 800°C, 900°C, and 1000°C for 5 hours	212
7.13	Percentage conversion of CO ₂ by Ru/Mn/Pr (5:30:65)/Al ₂ O ₃ calcined at various calcination temperatures for 5 hours	213
7.14	Percentage conversion of CO ₂ by Ru/Mn/Pr (5:30:65)/Al ₂ O ₃ calcined at 800°C with various base loading	215

7.15	Percentage conversion of CO ₂ by Ru/Mn/Pr (5:35:60)/Al ₂ O ₃ calcined at 800°C with various catalyst loading	217
7.16	Percentage conversion of CO ₂ by various loadings of ruthenium for Ru/Mn/Pr (5:30:65)/Al ₂ O ₃ catalyst at 800°C	218
7.17	Comparison of CO ₂ conversion for Ru/Mn/Pr (5:30:65)/Al ₂ O ₃ catalyst by using double reactor calcined at 800°C for 5 hours	219
7.18	Methane formation in in-situ reactions of methanation over Ru/Mn/Pr (5:30:65)/Al ₂ O ₃ catalyst at various calcination temperature	221
7.19	Levels of the optimization conditions for praseodymium catalyst	226
7.20	Experimental design for CO ₂ conversion and results response for praseodymium catalyst	227
7.21	ANOVA data (partial sum of squares) for response surface model (response: CO ₂ conversion)	228
8.1	Methane formation of in-situ methanation reactions over Ru/Mn/Ce (5:35:60)/Al ₂ O ₃ and Ru/Mn/Sm (5:35:60)/Al ₂ O ₃ catalyst	235
8.2	Methane formation of in-situ methanation reactions over Ru/Mn/Pr (5:30:65)/Al ₂ O ₃ catalyst	240

LIST OF FIGURES

FIGURE NO.	TITLE	PAGE
1.1	Percentage of CO ₂ emission from various activities in Malaysia	3
3.1	Frame of Work	36
3.2	Uncoated (a) and coated (b) of alumina support using cerium catalyst	39
3.3	Schematic diagram of Home-built micro reactor	39
3.4	Schematic diagram for the preparation of sample glass tube to be fixed in home-built micro reactor	40
3.5	Calibration graph of standard 99% pure methane	41
4.1	Representative of the FTIR spectra for the CO ₂ /H ₂ methanation reaction Ru/Mn/Sm (5:35:60)/Al ₂ O ₃ catalyst calcined at 400°C	54
4.2	Catalytic performance of M/Al ₂ O ₃ (M= Sm, Nd, Ce, Pr, Gd, La) catalyst calcined at 400°C for 5 hours	55
4.3	CO ₂ conversion over Mn/La with different ratio calcined at 400°C for 5 hours	56
4.4	CO ₂ conversion over Co/La with different ratio calcined at 400°C for 5 hours	56
4.5	CO ₂ conversion over Mn/Ce with different ratio calcined at 400°C for 5 hours	57
4.6	CO ₂ conversion over Co/Ce with different ratio calcined at 400°C for 5 hours	58
4.7	CO ₂ conversion over Mn/Sm with different ratio calcined at 400°C for 5 hours	58

4.8	CO ₂ conversion over Co/Sm with different ratio calcined at 400°C for 5 hours	59
4.9	CO ₂ conversion over Mn/Pr with different ratio calcined at 400°C for 5 hours	59
4.10	CO ₂ conversion over Co/Pr with different ratio calcined at 400°C for 5 hours	60
4.11	CO ₂ conversion over Mn/Nd with different ratio calcined at 400°C for 5 hours	60
4.12	CO ₂ conversion over Co/Nd with different ratio calcined at 400°C for 5 hours	61
4.13	CO ₂ conversion over Mn/Gd with different ratio calcined at 400°C for 5 hours	61
4.14	CO ₂ conversion over Co/Gd with different ratio calcined at 400°C for 5 hours	62
5.1	XRD diffractogram of Ru/Mn/Ce (5:35:60)/Al ₂ O ₃ catalyst calcined at various temperatures ; 400°C, 700°C, 800°C and 1000°C for 5 hours	75
5.2	XRD diffractogram of Ru/Mn/Ce (5:35:60)/Al ₂ O ₃ catalyst calcined at 1000°C with various based loading; 55%, 60%, and 65% for 5 hours	78
5.3	Wide scan of XPS spectrum obtained from fresh Ru/Mn/Ce (5:35:60)/Al ₂ O ₃ catalyst	82
5.4	High resolution Ce 3 <i>d</i> XPS spectrum obtained from fresh Ru/Mn/Ce (5:35:60)/Al ₂ O ₃ catalyst	83
5.5	High resolution O 1 <i>s</i> XPS spectrum obtained from fresh Ru/Mn/Ce (5:35:60)/Al ₂ O ₃ catalyst	84
5.6	High resolution Al 2 <i>p</i> XPS spectrum obtained from fresh Ru/Mn/Ce (5:35:60)/Al ₂ O ₃ catalyst	85
5.7	High resolution Mn 2 <i>p</i> XPS spectrum obtained from fresh Ru/Mn/Ce (5:35:60)/Al ₂ O ₃ catalyst	86
5.8	ESR spectra for Ru/Mn/Ce (5:35:60)/Al ₂ O ₃ catalyst calcined at 600°C, 700°C, and 800°C for 5 hours	88

5.9	H ₂ -TPR profile of Ru/Mn/Ce (5:35:60)/Al ₂ O ₃ at different calcination temperatures	90
5.10	CO ₂ -TPD curve of Ru/Mn/Ce (5:35:60)/Al ₂ O ₃ calcined at 700°C for 5 hours	92
5.11	FESEM micrpgraphs of Ru/Mn/Ce (5:35:60)/Al ₂ O ₃ catalyst calcined at a) 400°C, b) 600°C, c) 700°C, d) 800°C, and e) 1000°C for 5 hours in 50 000x magnification	94
5.12	EDX mapping of Ru/Mn/Ce (5:35:60)/Al ₂ O ₃ catalyst calcined at 600°C for 5 hours	96
5.13	EDX mapping of Ru/Mn/Ce (5:35:60)/Al ₂ O ₃ catalyst calcined at 700°C for 5 hours	97
5.14	EDX mapping of Ru/Mn/Ce (5:35:60)/Al ₂ O ₃ catalyst calcined at 800°C for 5 hours	98
5.15	Isotherm plot and pore size distribution of nitrogen adsorption for Ru/Mn/Ce (5:35:60)/Al ₂ O ₃ catalyst calcined at 600°C for 5 hours	100
5.16	Isotherm plot and pore size distribution of nitrogen adsorption for Ru/Mn/Ce (5:35:60)/Al ₂ O ₃ catalyst calcined at 700°C for 5 hours	101
5.17	Isotherm plot and pore size distribution of nitrogen adsorption for Ru/Mn/Ce (5:35:60)/Al ₂ O ₃ catalyst calcined at 800°C for 5 hours	101
5.18	TGA-DTA thermogram of as-synthesize of Ru/Mn/Ce (5:35:60)/Al ₂ O ₃ catalyst	103
5.19	FTIR spectra of Ru/Mn/Ce (5:35:60)/Al ₂ O ₃ catalyst calcined at a) 600°C, b) 700°C, and c) 800°C	104
5.20	CO ₂ conversion of cerium oxide catalyst calcined at different calcination temperatures for 5 hours, 7g catalyst	107
5.21	CO ₂ conversion of Ru/Mn/Ce (5:35:60)/Al ₂ O ₃ catalyst calcined at 700°C for 5 hours with various based loading, 7g catalyst	109

5.22	CO ₂ conversion of Ru/Mn/Ce (5:35:60)/Al ₂ O ₃ catalyst calcined at 700°C for 5 hours with various catalyst loadings	110
5.23	CO ₂ conversion of Ru/Mn/Ce (5:35:60)/Al ₂ O ₃ catalyst calcined at 700°C for 5 hours with various ruthenium loading, 7g catalyst	112
5.24	CO ₂ conversion of Ru/Mn/Ce (5:35:60)/Al ₂ O ₃ catalyst calcined at 700°C for 5 hours with double reactors	113
5.25	HPLC chromatogram of Ru/Mn/Ce (5:35:60)/Al ₂ O ₃ catalyst calcined at 700°C for 5 hours	116
5.26	Reproducibility test of Ru/Mn/Ce (5:35:60)/Al ₂ O ₃ catalyst calcined at 700°C for 5 hours, 7 g catalyst	117
5.27	Stability test on Ru/Mn/Ce (5:35:60)/Al ₂ O ₃ catalyst at 350°C reaction temperature	118
5.28	Regeneration test on Ru/Mn/Ce (5:35:60)/Al ₂ O ₃ catalyst at 700°C calcination temperature	119
5.29	Relationship of a) predicted and actual value and b) normal plot of residuals for cerium catalyst	124
5.30	Effect of calcination temperature and ratio for CO ₂ conversion, catalyst dosage of 5g	125
5.31	Effect of calcination temperature and catalyst dosage for CO ₂ conversion, ratio of 70%	126
5.32	Effect of ratio and catalyst dosage for CO ₂ conversion, calcination temperature of 700°C	127
5.33	Effect of ratio and calcination temperature for CO ₂ conversion, catalyst dosage = 6.94g	129
6.1	XRD diffractogram of Ru/Mn/Sm (5:35:60)/Al ₂ O ₃ catalyst calcined at various temperatures ; 400°C, 700°C, 900°C, 1000°C and 1100°C for 5 hours	131
6.2	XRD diffractogram of Ru/Mn/Sm (5:35:60)/Al ₂ O ₃ catalyst calcined at 1000°C with various based loading; 55%, 60%, and 65% for 5 hours	135

6.3	Wide scan of XPS spectrum obtained from fresh Ru/Mn/Sm (5:35:60)/Al ₂ O ₃ catalyst	137
6.4	High resolution O 1s XPS spectrum obtained from fresh Ru/Mn/Sm (5:35:60)/Al ₂ O ₃ catalyst	138
6.5	High resolution Al 2p XPS spectrum obtained from fresh Ru/Mn/Sm (5:35:60)/Al ₂ O ₃ catalyst	139
6.6	High resolution Mn 2p XPS spectrum obtained from fresh Ru/Mn/Sm (5:35:60)/Al ₂ O ₃ catalyst	140
6.7	High resolution Sm 3d XPS spectrum obtained from fresh Ru/Mn/Sm (5:35:60)/Al ₂ O ₃ catalyst	141
6.8	High resolution Ru 3p XPS spectrum obtained from fresh Ru/Mn/Sm (5:35:60)/Al ₂ O ₃ catalyst	142
6.9	ESR spectra for Ru/Mn/Sm (5:35:60)/Al ₂ O ₃ catalyst calcined at 900°C, 1000°C, and 1100°C for 5 hours	144
6.10	H ₂ -TPR profile of Ru/Mn/Sm (5:35:60)/Al ₂ O ₃ at different calcination temperatures	146
6.11	CO ₂ -TPD curve of Ru/Mn/Sm (5:35:60)/Al ₂ O ₃ calcined at 1000°C for 5 hours	148
6.12	FESEM micrographs of Ru/Mn/Sm (5:35:60)/Al ₂ O ₃ catalyst calcined at a) 400°C, b) 700°C, c) 900°C, d) 1000°C, and e) 1100°C for 5 hours in 50 000x magnification	150
6.13	EDX mapping of Ru/Mn/Sm (5:35:60)/Al ₂ O ₃ catalyst calcined at 900°C for 5 hours	152
6.14	EDX mapping of Ru/Mn/Sm (5:35:60)/Al ₂ O ₃ catalyst calcined at 1000°C for 5 hours	153
6.15	EDX mapping of Ru/Mn/Sm (5:35:60)/Al ₂ O ₃ catalyst calcined at 1100°C for 5 hours	154
6.16	Isotherm plot and pore size distribution of nitrogen adsorption for Ru/Mn/Sm (5:35:60)/Al ₂ O ₃ catalyst calcined at 900°C for 5 hours	156

6.17	Isotherm plot and pore size distribution of nitrogen adsorption for Ru/Mn/Sm (5:35:60)/Al ₂ O ₃ catalyst calcined at 1000°C for 5 hours	157
6.18	Isotherm plot and pore size distribution of nitrogen adsorption for Ru/Mn/Sm (5:35:60)/Al ₂ O ₃ catalyst calcined at 1100°C for 5 hours	157
6.19	TGA-DTA thermogram of as-synthesize of Ru/Mn/Sm (5:35:60)/Al ₂ O ₃ catalyst	158
6.20	FTIR spectra of Ru/Mn/Sm (5:35:60)/Al ₂ O ₃ catalyst calcined at a) 900°C, b) 1000°C, and c) 1100°C	160
6.21	CO ₂ conversion of samarium oxide catalyst calcined at different calcination temperatures for 5 hours, 7g catalyst	163
6.22	CO ₂ conversion of Ru/Mn/Sm (5:35:60)/Al ₂ O ₃ catalyst with various based loading at 1000°C calcination temperature for 5 hours, 7 g catalyst	165
6.23	CO ₂ conversion of Ru/Mn/Sm (5:35:60)/Al ₂ O ₃ catalyst with various catalyst loadings calcined at 1000°C for 5 hours	166
6.24	CO ₂ conversion of Ru/Mn/Sm (5:35:60)/Al ₂ O ₃ catalyst calcined at 1000°C for 5 hours with various ruthenium loading, 7 g catalyst	168
6.25	CO ₂ conversion of Ru/Mn/Sm (5:35:60)/Al ₂ O ₃ catalyst calcined at 1000°C for 5 hours with double reactors	169
6.26	HPLC chromatogram of the product obtained using Ru/Mn/Sm (5:35:60)/Al ₂ O ₃ catalyst calcined at 1000°C for 5 hours	172
6.27	Reproducibility test of Ru/Mn/Sm (5:35:60)/Al ₂ O ₃ catalyst calcined at 1000°C for 5 hours, 7 g catalyst	173
6.28	Stability test on Ru/Mn/Sm (5:35:60)/Al ₂ O ₃ catalyst at 350°C reaction temperature	174
6.29	Regeneration test on Ru/Mn/Sm (5:35:60)/Al ₂ O ₃ catalyst at 1000°C calcination temperature	175

6.30	Relationship of a) predicted and actual value and b) normal plot of residuals for samarium catalyst	180
6.31	Effect of calcination temperature and ratio for CO ₂ conversion, catalyst dosage of 5g	181
6.32	Effect of calcination temperature and catalyst dosage for CO ₂ conversion, ratio of 70%	182
6.33	Effect of ratio and catalyst dosage for CO ₂ conversion, calcination temperature of 1000°C	183
6.34	Effect of ratio and calcination temperature for CO ₂ conversion, catalyst dosage = 6.76g	185
7.1	XRD diffractogram of Ru/Mn/Pr(5:30:65)/Al ₂ O ₃ catalyst calcined at various temperatures ; 400°C, 700°C, 800°C, 900°C and 1000°C for 5 hours	187
7.2	XRD diffractogram of Ru/Mn/Pr (5:30:65)/Al ₂ O ₃ catalyst calcined at 800°C with various based loading; 55%, 60%, and 65% for 5 hours	189
7.3	Wide scan of XPS spectrum obtained from fresh Ru/Mn/Pr (5:30:65)/Al ₂ O ₃ catalyst	191
7.4	High resolution O 1s XPS spectrum obtained from fresh Ru/Mn/Pr (5:30:65)/Al ₂ O ₃ catalyst	192
7.5	High resolution Al 2p XPS spectrum obtained from fresh Ru/Mn/Pr (5:30:65)/Al ₂ O ₃ catalyst	193
7.6	High resolution Mn 2p XPS spectrum obtained from fresh Ru/Mn/Pr (5:30:65)/Al ₂ O ₃ catalyst	194
7.7	High resolution Pr 3d XPS spectrum obtained from fresh Ru/Mn/Pr (5:30:65)/Al ₂ O ₃ catalyst	195
7.8	ESR spectra for Ru/Mn/Pr (5:30:65)/Al ₂ O ₃ catalyst calcined at 800°C, 900°C, and 1000°C for 5 hours	197
7.9	H ₂ -TPR profile of Ru/Mn/Pr (5:30:65)/Al ₂ O ₃ at different calcination temperatures	199
7.10	CO ₂ -TPD curve of Ru/Mn/Pr (5:30:65)/Al ₂ O ₃ calcined at 1000°C for 5 hours	200

7.11	FESEM micrographs of Ru/Mn/Pr (5:30:65)/Al ₂ O ₃ catalyst calcined at a) 400°C, b) 700°C, c) 800°C, d) 900°C, and e) 1000°C for 5 hours in 50 000x magnification with scale bar 1.00µm	202
7.12	EDX mapping of Ru/Mn/Pr (5:30:65)/Al ₂ O ₃ catalyst calcined at 800°C for 5 hours	204
7.13	EDX mapping of Ru/Mn/Pr (5:30:65)/Al ₂ O ₃ catalyst calcined at 900°C for 5 hours	205
7.14	EDX mapping of Ru/Mn/Pr (5:30:65)/Al ₂ O ₃ catalyst calcined at 1000°C for 5 hours	206
7.15	Isotherm plot and pore size distribution of nitrogen adsorption for Ru/Mn/Pr (5:30:65)/Al ₂ O ₃ catalyst calcined at 800°C for 5 hours	208
7.16	Isotherm plot and pore size distribution of nitrogen adsorption for Ru/Mn/Pr (5:30:65)/Al ₂ O ₃ catalyst calcined at 900°C for 5 hours	209
7.17	Isotherm plot and pore size distribution of nitrogen adsorption for Ru/Mn/Pr (5:30:65)/Al ₂ O ₃ catalyst calcined at 1000°C for 5 hours	209
7.18	TGA-DTA thermogram of as-synthesize of Ru/Mn/Pr (5:30:65)/Al ₂ O ₃ catalyst	210
7.19	FTIR spectra of Ru/Mn/Pr (5:30:65)/Al ₂ O ₃ catalyst calcined at a) 800°C, b) 900°C, and c) 1000°C	212
7.20	CO ₂ conversion of Ru/Mn/Pr (5:30:65)/Al ₂ O ₃ catalyst calcined at different calcination temperatures for 5 hours, 7g catalyst	215
7.21	CO ₂ conversion of Ru/Mn/Pr (5:30:65)/Al ₂ O ₃ catalyst with various based loading at 800°C calcination temperature for 5 hours, 7 g catalyst	217
7.22	CO ₂ conversion of Ru/Mn/Pr (5:30:65)/Al ₂ O ₃ catalyst with various catalyst loadings calcined at 800°C for 5 hours	218

7.23	CO ₂ conversion of Ru/Mn/Pr (5:30:65)/Al ₂ O ₃ catalyst calcined at 800°C for 5 hours with various ruthenium loadings, 7 g catalyst	220
7.24	CO ₂ conversion of Ru/Mn/Pr (5:30:65)/Al ₂ O ₃ catalyst calcined at 800°C for 5 hours with double reactor	221
7.25	Reproducibility test of Ru/Mn/Pr (5:30:65)/Al ₂ O ₃ catalyst calcined at 800°C for 5 hours, 7 g catalyst	223
7.26	Stability test on Ru/Mn/Pr (5:30:65)/Al ₂ O ₃ catalyst at 350°C reaction temperature	225
7.27	Regeneration test on Ru/Mn/Pr (5:30:65)/Al ₂ O ₃ catalyst at 1000°C calcination temperature	226
7.28	Relationship of a) predicted and actual value and b) normal plot of residuals for praseodymium catalyst	230
7.29	3D (a) and contour plot (b) of CO ₂ conversion versus calcination temperature and ratio. Fixed catalyst dosage = 5g	231
7.30	3D (a) and contour plot (b) of CO ₂ conversion versus calcination temperature and catalyst dosage. Fixed catalyst dosage = 75%	232
7.31	3D (a) and contour plot (b) of CO ₂ conversion versus ratio and catalyst dosage. Fixed calcination temperature = 900°C	233
7.32	3D (a) and contour plot (b) of CO ₂ conversion versus ratio and calcination temperature.	234
8.1	FTIR spectra of Ru/Mn/Sm (5:35:60)/Al ₂ O ₃ at reaction temperature, a) 100°C, b) 200°C, c) 250°C, d) 300°C, e) 350°C, and f) 400°C calcined at 1000°C for 5 hours	237
8.2	The proposed mechanism for methanation reaction of CO ₂ and H ₂ over Ru/Mn/Ce (5:35:60)/Al ₂ O ₃ and Ru/Mn/Sm (5:35:60)/Al ₂ O ₃ catalysts	239
8.3	FTIR of catalytic activity of Ru/Mn/Sm (5:35:60)/Al ₂ O ₃ calcined at 1000°C during mechanistic study	240

8.4	FTIR spectra of Ru/Mn/Pr (5:30:65)/Al ₂ O ₃ at reaction temperature, a) 100°C, b) 200°C, c) 250°C, d) 300°C, e) 350°C, and f) 400°C calcined at 800°C for 5 hours	242
8.5	The proposed mechanism for methanation reaction of CO ₂ and H ₂ over Ru/Mn/Pr (5:30:65)/Al ₂ O ₃ catalysts	243
8.6	FTIR of catalytic activity of Ru/Mn/Pr (5:30:65)/Al ₂ O ₃ calcined at 800°C during mechanistic study	243

LIST OF ABBREVIATIONS

ABS	Absorbance
BET	Brunnauer, Emmet and Teller
BJH	Barret-Joyner-Halenda
Btu	British thermal unit
CHA	Concentric hemispherical analyzer
Cu K α	X-ray diffraction from Copper K energy levels rate of conversion (percentage)
d	Pore diameter
DTA	Differential Thermal Analysis
EDX	Energy Dispersive X-ray Analysis
ESR	Electron Spin Resonance
eV	Electronvolt
FESEM	Field Emission Scanning Electron Microscope
FID	Flame Ionization Detector
FTIR	Fourier Transform Infrared
GC	Gas Chromatography
ΔH	Enthalpy change
hr	Hour
h ν	Photon's energy
IUPAC	International Union of Pure and Applied Chemistry
LNG	Liquefied Natural Gas
MgK α	X-ray diffraction from Magnesium K energy levels rate of conversion (percentage)
MS	Mass Spectroscopy
MW	Molecular Weight

P/P_0	Relative pressure; obtained by forming the ratio of the equilibrium pressure and vapour pressure P_0 of the adsorbate at the temperature where the isotherm is measured
PDF	Powder Diffraction File
SMSI	Strong metal support interaction
tcf	Trillion cubic feet
TGA	Thermogravimetry Analysis
XPS	X-ray Photoelectron Spectroscopy
XRD	X-ray Diffraction
a_0	Cell constant
θ	Half angle of diffraction beam
λ	Wavelength

LIST OF APPENDICES

Appendix	TITLE	PAGE
A	Calculation of atomic weight percentage ratio of element in catalyst preparation	272
B	Preparation of alumina supported cerium, samarium, praseodymium oxide based catalysts and its ratio	273
C	Calculation of methane percentage	274
D	Schematic diagram of Home-built micro reactor connected using two isothermal furnaces	275
E	Standard of methanol via HPLC analysis	276
F	Methanol analysis via HPLC over Ru/Mn/Pr (5:30:65)/Al ₂ O ₃	277
G	Publications and presentations	278
H	Awards	280

CHAPTER 1

INTRODUCTION

1.1 Background of Study

Natural gas is a vital component of the world's supply of energy. It is one of the cleanest, safest, and most useful of all energy sources. Natural gas affords clean burning and emits lower levels of potentially harmful by-products into the air (Curry, 1981). Natural gas is considered 'dry' when it is almost pure methane, having most of the other commonly associated hydrocarbons removed. When other hydrocarbons are present, the natural gas is 'wet'.

Naturally, natural gas is produced by the anaerobic decay of non-fossil organic materials. The primary component of natural gas is methane (CH_4). It also contains heavier hydrocarbon gaseous such as ethane (C_2H_6), propane (C_3H_8) and butane (C_4H_{10}). Besides that, it also contains other toxic and acidic gaseous like CO_2 , N_2 , mercury (Hg) and H_2S as investigated by Curry, (1981).

Malaysia is currently a net exporter of natural gas and is the world's third largest exporter after Algeria and Indonesia. In 2001, the country exported 49.7% of its natural gas production in the form of liquefied natural gas (LNG) to Japan which is the world biggest user, as well as to the Republic of Korea and Taiwan under long-term contracts. The other 50.3% of Malaysia's natural gas was delivered to the gas processing plants (Radler, (2003)).

However, Malaysia's natural gas consists of several gaseous and impurities such as non-hydrocarbon gases which includes carbon dioxide. The presence of these impurities could make the natural gas fall under "sour natural gas" as they can cause the formation of corrosive compounds such as carbonic acid in the presence of water according to Speight, (2007). Sour gas also contains hydrogen sulfide, whereas sweet gas contains very little, if any, hydrogen sulfide. This will result in lowering the price of natural gas in worldwide market as well as causing difficulties for its distribution to the market.

The chemical composition of Malaysia's natural gas before it is refined is shown in Table 1.1 (*Van Rossum, 1986*).

Table 1.1 Chemical composition of Malaysia's natural gas

Chemical Name	Percentage (%)
Methane (CH ₄)	40–50
Ethane (C ₂ H ₆)	5–10
Propane (C ₃ H ₈)	1–5
Hydrogen Sulphide (H ₂ S)	1–5
Carbon Dioxide (CO ₂)	20–30

Consequently, due to the impurities of the natural gas, especially CO₂, the percentage of CO₂ gases in the Malaysia and world have increased year by year. Figure 1.1 shows the percentage of CO₂ emission based on various activities in Malaysia (*Yusof et al., 2010*). Fossil fuels supply more than 98% of the world's energy needs, though unfortunately, the resulting combustions from the utilization of fossil fuels are one of the major sources of the green house gas CO₂.

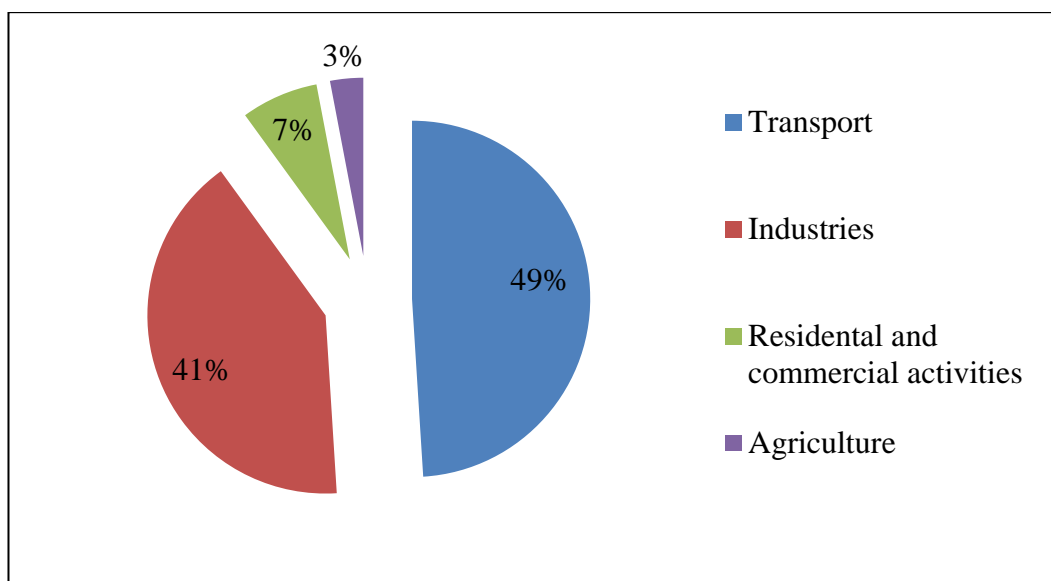


Figure 1.1 Percentage of CO₂ emission from various activities in Malaysia (Yusof *et al.*, 2010).

The main objective of the United Nations Framework Convention on Climate Change (UNFCCC) is the stabilization of greenhouse gas concentrations in the atmosphere at a certain level to avoid the interference of dangerous anthropogenic with the climate system (Strakey *et al.*, (1975)). The Protocol was adopted by Parties to the UNFCCC in 1997, and entered into force in 2005 as also been reported by Md Yassin (1987). As part of the Kyoto Protocol, which is an international treaty that sets binding obligations on industrialized countries to reduce emissions of greenhouse gases, many developed countries have agreed to a legal binding that required them to reduce their emissions of greenhouse gases in two commitment periods. The first commitment period applies to emissions in between 2008-2012, while the second commitment period applies to emissions flanked by the year 2013-2020. The protocol was amended in 2012 to accommodate the second commitment period (Raupach *et al.*, (2007)) but this amendment has not (as of January 2013) entered into legal force (James and Mark (2009)).

For the developed countries to trade their commitments under Kyoto Protocol, they are allowed to trade their emission quotes among themselves and could receive credit for financing emission reduction as been reported by Zou *et al.*, (2005). A carbon credit is a term for any tradable certificate or permit representing

the right to emit one tonne of carbon dioxide or the mass of another greenhouse gas with a carbon dioxide equivalent to one tonne of carbon dioxide (Mc Naught and Wilkinson (1997)). The aim for carbon credit is to allow market mechanisms to drive industrial and commercial processes in the direction of low emissions or less carbon intensive approaches than those used when there is no cost to emit carbon dioxide and other GHGs into the atmosphere.

Therefore, it is necessary to develop technologies that will allow the utilization of fossil fuels while reducing the emissions of green house gases. Green technology is an alternative that reduces fossil fuels and demonstrates less damage to human, animal and plant. Green technologies include such area as renewable energy sources, waste management, and remediation of environmental pollutants, sewage treatment and recycling together with water purification, as discussed by Ismail and Ishak (2011). Commercial CO₂ capture technology that exists today is very expensive and energy intensive. Improved technologies for CO₂ capture are necessary in order to achieve low energy penalties. Pressure swing adsorption (PSA) is one of the potential techniques that could be applicable for removal of CO₂ from high pressure gas streams such as those encountered in Integrated Gasification Combined Cycle (IGCC) systems (Haldor (2005)).

At present, Malaysia has already committed under UNFCCC to implement and regularly update to mitigate climate change by reducing the emission of all greenhouse gases. Oil and gas have been the main sources of energy in Malaysia which projected to upward trend from 1244 Petajoule (PJ) in 2000 to an estimated 2218 PJ in 2010. Currently, the energy mix supply is made of gas (70%), coal (22%), oil (2%) and hydropower (6%). A new project to combust methane at Seelong Sanitary Landfill is expected to reduce CO₂ emission more than 100,000 tonnes a year and the Jendarata Steam and power plant and Jendarata Palm Oil mill have the expected combined CO₂ emission reduction of more than 30,000 tonnes annually as reported by Lau *et al.*, (2009) and Razak and Ramli (2008).

1.2 Gas Purification Process

Gas processing is necessary to ensure that the natural gas intended for use is clean-burning and environmentally acceptable. One of the most important procedures of gas processing is the removal of carbon dioxide and hydrogen sulfide. The removal of acid gases (CO_2 , H_2S and other sulfur components) from natural gas is often referred to as gas sweetening process.

Amine treating is one of the processes used to remove CO_2 and H_2S from natural gas. Amine has a natural affinity for both CO_2 and H_2S which allows it to be very efficient and effective in the removal process. When CO_2 reacts with water, it creates carbonic acid which is corrosive. CO_2 also reduces the BTU value of gas and the gas is unmarketable as it reaches concentrations of more than 2% or 3%. H_2S is an extremely toxic gas that is also tremendously corrosive to equipment. Amine plant design is based on proven amine regeneration technology and incorporates several patent-pending processes to improve the reliability and ease of operation. This process has many advantages, especially in regards to its lower installation and removal costs. Amine sweetening processes remove these contaminants so that the gas is marketable and suitable for transportation (William and David (2005)). However, this method has a few limitation which are complex and have high capital, operating, and installation costs; a relatively high fuel cost and potential environmental issues.

Another method is PRISM membrane from Air Product Company that can be used as a gas scrubber for natural gas. The CO_2 gas needs to be removed to improve the heating value of the gas and to meet the pipeline specification. The benefits of this process include minimal maintenance cost, no involvement of hazardous chemical, as well as being easy to be installed and operated. Prism membranes will effectively separate carbon dioxide from hydrocarbon vapours (Michael, 2010). However, the performance is highly dependent on CO_2 content in the raw feed gas, CO_2 specification in product, supply pressure; permeate pressure, and operating temperature as investigated by Stookey, (1986).

Membrane separation process performs on the principle of selective gas permeation. When gas mixture is introduced to membrane, component of gas permeated along into membrane material and diffuses through the membrane material. Gas treating membrane provides a safe and efficient option for water vapour and carbon dioxide from natural gas. Components with higher permeation rates (such as CO_2 , H_2 , and H_2S) will permeate faster through the membrane module than components with lower permeation rates (such as N_2 , Cl , C_2H_6 and heavier hydrocarbons). The primary driving force of the separation is the differential partial pressure of the permeating component. Therefore, the pressure difference between the feed gas and permeate gas and the concentration of the permeating component determine the product purity and the amount of carbon dioxide membrane surface required.

For years, the iron sponge type process has widely been used by the industry to treat sour gas. An iron sponge is a cylinder shaped vessel containing iron oxide treated wood chips. The iron oxide reacts with hydrogen sulfide to form relatively inert iron sulfide and water. However, the iron oxide does not last forever and the effectiveness of the wood chips will eventually fall below acceptable standards. When this occurs, the iron sponge must be taken off-line and the old wood chips are replaced by a new fully charged material. There are increase concerns of the environmental impact associated with the disposal of spent material and labor costs for replacement. These would increase the number of scavengers with better disposal properties.

Clauss process is the most significant method known in the removal of sulphur from hydrogen sulphide gaseous. The multi-step Claus process recovers sulfur from the hydrogen sulfide gaseous found in raw natural gas and for over 25% H_2S contents. The Claus process contains two steps which is thermal and catalytic. In the thermal step, hydrogen sulfide-laden gas reacts in a substoichiometric combustion at temperatures above 850°C such that elemental sulfur precipitates in the downstream process gas cooler. Usually, 60 to 70% of the total amounts of elemental sulfur produced in the process are obtained in the thermal process step. Then the process continues with catalytic processing which involves the use of

activated aluminiums (III) or titaniums (IV) oxide and serves to boost the sulfur yield. More hydrogen sulfide (H_2S) reacts with the SO_2 during combustion in the reaction furnace in the Claus reaction, and the product is in gaseous, and elemental sulfur.

Even though several methods as mentioned above have been developed for the removal of acid gases from the natural gas composition, these methods have several general drawbacks such as its high cost and production of high heat of reaction. Therefore, a new method was focused in this study which is a more promising method that involves the utilization of the catalytic conversion system by using supported mixed metal oxides catalyst.

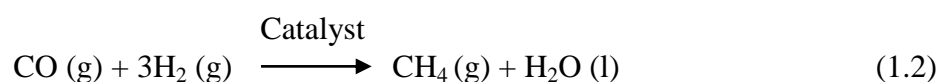
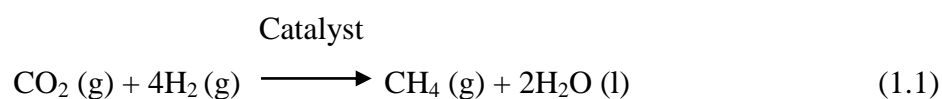
1.3 Catalytic Methanation

Methanation is a physical-chemical process to generate methane from a mixture of various gases out of biomass fermentation or thermal-chemical gasification as defined by Ponee (1978). Meanwhile, catalytic methanation reaction refers to a process for removing carbon monoxide and carbon dioxide from gas stream for producing methane by using catalyst (Mills and Fred, 1974).

The essential requirement for the correct selection of the metal oxide catalyst system is its ability to accept and to activate CO_2 and H_2S . The acidic nature of CO_2 and H_2S requires the employment of a catalytic system with Lewis basic properties such as Group VIII metals. The major reason for the much slower development of the catalytic science of mixed metal oxide is its significant complexity compared with single metal based catalysts such as the possible presence of multiple oxidation states, variable local coordination, coexisting bulk and surface phases as well as different surface termination functionalities such as M-OH , M=O or M-O as mentioned by Ertesva, *et al.*, (2005).

The relative activity of various transition metals for methanation and desulphurization can be determined at atmospheric pressure under the conditions in which most other hydrocarbon molecules are likely to form. In a previous research by Vannice (1987), the order of decreasing activity of transition metals was Fe > Ni > Co and the activation energy for methanation of CO₂ and H₂ was in the range of 23-25 kcal/mole.

In natural gas purification, the conversion of carbon dioxide to methane is an important process. To form methane (CH₄), hydrogen gas is used along with carbon dioxide and carbon monoxide gas (from incomplete methanation reaction) through methanation process as shown in Equation 1.1 and 1.2 below:



The catalytic reactions depend on the interactions between the active sites and the reactants, in a series of adsorption-desorption and surface reaction steps, as well as heat and mass transfer (Saluko, 2005).

Since the catalytic process through methanation reaction provides the most effective way to remove CO₂ and H₂S in the natural gas, therefore, the present study was conducted in order to develop a catalyst based on lanthanide oxide by modifying the dopants using noble metal in order to fully remove these sour gases at high conversion percentage and, possibly, at low temperature. Lanthanide oxide was used because the chemistry of the lanthanides differs from the main group elements and the transition metals. The nature of the 4f orbitals and its ions has slightly different radii, leading to a small difference in solubility as reported by Holden and Coplen (2004).

1.4 Response Surface Methodology

Response surface methodology (RSM) is a set of techniques used in the empirical study of relationship between one or more responses and a group of variables (Cornell, 1990). RSM is useful for developing, modelling, improving, and optimizing the important response variable in an experiment run through the analyzing of programs. RSM comprises of three techniques or methods (Montgomery, 1999): (1) statistical experimental design, particularly the two level factorial or factorial design, (2) regression modeling techniques, and (3) optimization for optimum operating conditions through experimental methods. The most common application of RSM is in industrial, biological and clinical science, social science, food science, and physical and engineering sciences. According to research conducted by Myers *et al.*, (1992), the first-order model was motivated by Box and Hunter, (1954) by using *orthogonal design*. The second-order model, which is most frequently used, consists of the 3^k *factorial*, *central composite designs (CCD)*, and *Box-Behnken design*. An approximate of the relationship between y and the independent variables for second-order model is shown in Equation 1.3 and 1.4 where x_i and x_j are the design variables and β are the tuning parameters.

$$y = \beta_0 + \beta_1 x_1 + \cdots + \beta_k x_k + \varepsilon \quad (1.3)$$

$$y = \beta_0 + \sum_{i=1}^k \beta_i x_i + \sum_{i=1}^k \beta_{ii} x_i^2 + \sum_{i<j} \beta_{ij} x_i x_j + \varepsilon \quad (1.4)$$

The CCD is ideal for sequential experimentation and allows a reasonable amount of information for testing lack of fit while not involving an unusually large number of design points (Joglekar and May, (1987)). Alternatively, Box-Behnken presents some advantages such as requiring few experimental points for its application (three levels per factor) and high efficiency as discussed by Khuri and Mukhopadhyay, (2010). The use of Box-Behnken design is popular in industrial research because it is an economical design and requires only three levels for each factor where the settings are -1, 0, and 1. Recently, more emphasis for an improvement in response instead of finding the optimum response has been placed by chemical and processing fields (Myers *et al.*, 1992).

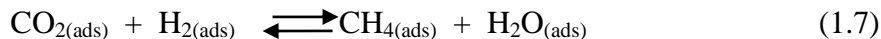
1.5 Mechanism of Methanation Reaction Process

The CO₂/H₂ methanation reaction follows the Langmuir Hinshelwood (LH) mechanism which involves initially the adsorption of CO₂ and H₂ gases on the catalyst surface. Adsorption, desorption and surface diffusion play an essential role in LH mechanism. Four assumptions of Langmuir-Hinshelwood are: (1) the surface of the adsorbent is uniform, (2) adsorbed molecules do not interact, (3) all adsorption occurs through the same mechanism, and (4) at the maximum adsorption, only a monolayer is formed.

Therefore, it might be expected that the reaction rate should depend on the surface coverage of both species. Moreover, the dissociation of adsorbed H₂ molecule results in the formation of active H atom species, followed by dissociation of CO₂ molecule. This theory was supported by Solymosi *et al.*, (1981), who stated that CO₂ dissociation on supported precious metal catalysts using a conventional pulse reaction was promoted by the presence of H and CH_x fragments on a catalyst surface. They also proposed that CO₂ adsorption and subsequent dissociation on transition metals proceed through electron transfer from a metal to a CO₂ molecule to form anion radical species. Therefore, the adsorbed species attains a lower energy state once it has been adsorbed to the metal, thus lowering the activation barrier between the gas phase species and the support-adsorbed species. Afterward, the active H atom species attaches to the O atom to form water molecule and this process continuous until the carbon atom is fully attached with H atom to form methane.

According to Equation 1.5, carbon dioxide is reacting with the catalyst surface, (S) by chemisorptions and creates an active species that adsorbed onto catalyst surface. This is followed by hydrogen molecule that also reacts with catalyst surface by chemisorptions and adsorbed onto catalyst surface as an active species. Both active species than react each other to produce products that is methane and water.

For the simplest possible reaction, methanation process can be described as shown in Equation 1.5 to 1.9.



*S = Catalyst Surface

(ads) = adsorption of molecule on the catalyst surface

(desorp) = desorption of molecule on the catalyst surface

1.6 Statement of Problem

In Malaysia, population in urbanized area has been increasing rapidly and at the same time, demands for certain types of product by have increased in order to meet the current demands of the society. Modern society is highly dependent on vehicles such as cars, trucks and railways. Emissions from the vehicles rely mostly on burning fossil fuel, thus contributing to the many predominant green house gases (CO_2 , SO_2 , NO_2) emitted into the air either locally or globally. Carbon dioxide is the most significant green house gas produced from the transportation activities and the effects brought by it is attributed to the global warming phenomenon if adequate controls or mitigation measures are not taken as investigated by Yusof *et al.*, (2010).

The natural gas contains the most significant impurities, which are carbon dioxide (CO_2) and hydrogen sulphide (H_2S). Due to the impurities of CO_2 and H_2S , the natural gas will have lower quality and worldwide price. The reaction of CO_2 and H_2S with water could result into a highly corrosive acid which could rapidly destroy the pipelines and equipment as well as reducing the lifetime of equipment (Dortmundt *et al.*, 1999). H_2S itself is a colorless and flammable gas. It smells like rotten eggs that is toxic at extremely low concentration and can cause the loss of a

human's sense of smell. Therefore, these gaseous need to be removed in order to prevent or minimize the release of hazardous gases into the environment. This will help to reduce problems such as acid rain, ozone layer depletion or greenhouse effect. Hence, suitable methods are needed to overcome this problem.

Many methods on conversion of CO₂ such as amine treating, membrane separation, and others have been developed and investigated by researchers. However, these methods have several drawbacks such as low selectivity, high cost, and most importantly, the methods only work in the presence of CO₂ ≤ 10%. As Malaysia's natural gas contains ≥ 23% of CO₂ most of these methods are inapplicable in the efforts to convert the country's natural gases. Therefore, an alternative method is needed that is more economical and environmental-friendly.

Recently, an alternative method has been developed which is the catalytic conversion of CO₂ *via* methanation reaction. This method removes the toxic CO₂ gas and produces valuable methane simultaneously. It is also an economical method since the catalysts can be recycled, and it is also environmentally friendly as it does not emit any toxic gas into the air while the reaction takes place.

From previous study, most catalysts used were nickel, cobalt, ruthenium, and iron deposited on an alumina support for CO₂/H₂ methanation technique. However, these catalysts are very sensitive towards chemical attack, thus the performance of catalysts was not promising due to lower conversion of CO₂ in methanation process. Therefore, lanthanide oxide doped with noble metal was used in this study in order to overcome these problems by increasing the percentage conversion of CO₂ at lower reaction temperature. The potential of lanthanide oxide has been widely used as a based catalyst in ethanol reforming, adsorbent for desulfurization in realistic fuel processor, polymerization, ammonia synthesis, oxygen assisted water gas-shift, and HCOOH hydrogenation.

1.7 Objectives

Based on the problem statement which was focused on methanation reaction and the efforts to find the best catalysts for the conversion of CO₂ gas and production of higher methane, several objectives for this study were developed. The objectives of this research are as follow:-

1. To synthesize, characterize, and test the catalytic activity of supported lanthanide oxide doped manganese and cobalt with ruthenium as co-dopant catalysts for carbon dioxide methanation using fixed bed home-built micro reactor coupled with FTIR.
2. To optimize the catalysts preparation by various calcination temperatures, ratio based loadings and catalyst dosage ratio in the catalytic testing by response surface methodology.
3. To regenerate the spent catalysts from the reaction by running under O₂ flow at 100°C for 1 hours.
4. To propose the reaction mechanism through the analysis on the metal oxide surface and flue gas mixture.

1.8 Significance of Study

The increasing carbon dioxide and other green house gases content in Malaysia which contributes to global warming must be treated. The most significant reason that contributes to CO₂ emission is from transportations and chemical industries. Natural gas contains 23% of CO₂ gas that contributes to acid rain phenomena when it reacts with water. Therefore, CO₂ gas must be remove via methanation process which offers a green and clean technology to convert it into valuable methane gas. The methane produced can be used as fuel and in the case of natural gas, will improve the gas quality. This process is low cost and the catalyst used can be recycled. Lanthanide metals were used as the alternative catalysts and

are expected to be in low price, highly effective in reaction and can be highly activated at low temperature.

1.9 Scope of Study

In this research, lanthanide (samarium, cerium, praseodymium, lanthanum, neodymium, and gadolinium) oxides were used as catalyst's based while the dopants used were manganese and cobalt nitrate salt as precursor. The preparation of catalyst was conducted by incipient wetness impregnation method. Then the catalytic activity testing was conducted by using simulated natural gas and was carried out by the mixing of hydrogen and carbon dioxide gases (4:1) in a house-built micro reactor. The optimization parameters was done by Box-Behnken design with three critical parameters which are calcination temperature, ratio based loadings and catalyst dosage. The mechanistic study was conducted using Ru/Mn/Ce (5:35:60)/Al₂O₃, Ru/Mn/Sm (5:35:60)/Al₂O₃ and Ru/Mn/Pr (5:35:60)/Al₂O₃ catalysts using FTIR, GC and HPLC. The characterizations of catalyst were conducted by using various analytical techniques such as TGA-DTA, FESEM-EDX, XPS, ESR, TPR, XRD, FTIR, and NA techniques. The detailed research study is summarized in Figure 3.1.

REFERENCES

- Ab Halim A.Z. Ali R. and Wan Abu Bakar W.A. (2015). CO₂/H₂ methanation over M*/Mn/Fe-Al₂O₃ (M*= Pd, Rh, and Ru) catalysts in natural gas: Optimization by response surface methodology-central composite design. *Clean Technologies and Environmental Policy*. **17**(3). 627-636.
- Agrafiotis C. Tsetsekou A. Stournaras C.J. Julbe A. Dalmazio L. Guizard C. Boretto G. De Benedetti M. and Parussa F. (2011). Evaluation of sol-gel methods for the synthesis of doped-ceria environmental catalysis systems. Part II catalytic activity and resistance to thermal aging. *Applied Catalysis B: Environmental*. **34**. 149-159.
- Ali, A. M.; Suzuki, Y.; Inui, T.; Kimura, T.; Hamid, H. & Al-Yami, M. A. (2000), Hydrocracking Activity of Noble Metal Modified Clay-Based Catalysts Compared with a Commercial Catalyst. *Journal of Power Source*, **142**, 70–74.
- Anderson J.S. and Gallagher. (1963). The oxidation of praseodymium oxide. Part I chemisorptions on praseodymium oxide. *J. Chem. Soc.* 52-61.
- Araki M. and Ponec V. (1976). Methanation of Carbon Monoxide on Nickel and Nickel-copper Alloys. *Journal of Catalysis*. **44**. 439-448.
- Atichat W. Worapot I. Warangkhan S. Sorod C. Supunee J. and Chai Y.T. (2010). Pore size distribution of carbon with different probe molecules. *Engineering Journal*. **14**(3). 45-56.
- Bahgat A.A. Shisha E.E. and Sabry A.I. (1987). Physical properties of some rare earth tellurite glasses. *Journal of material Sciences* **22**(4). 1323.
- Bartholomew. Calvin H. (2011). Carbon Deposition in Steam Reforming and Methanation *Applied catalysis A: General*. **212**, 17-60.

- Bao X. Jiang Z. Zhou W. Tan D. Zhai R. (2004). Evidence for perimeter sites over SmOx-modified Rh(100) surface by CO chemisorption. *Surface Science*. **565**. 269-278.
- Beuls A. Swalus C. Jacqiemmin M. Heyen G. Kavelovic A. Ruiz P. (2011). Methanation of CO₂: Further insight into the methanation over Rh/Al₂O₃ catalyst. *Applied Catalysis B: Environmental*. **113-114**. 2-10.
- Borgschulte A. Gallandat N. Probst B. Suter R. Callini E. Ferri D. Arroyo Y. Erni R. Geerlings H. and Zittel A. (2013). Sorption enhanced CO₂ methanation. *Phys.Chem.Chem.Phys.* **15**. 9620-9625.
- Bosque-Sendra J.M. Pescarolo S. Cuadros-Rodríguez L. (2001). Optimizing analytical methods using sequential response surface methodology: Application to the pararosaniline determination of formaldehyde. *J.Anal Chem.* **36**. 715-718.
- Boukis N. Diem V. Habicht W. and Dinjus E. (2003). Methanol reforming in supercritical water. *Ind. Eng. Chem. Res.* **42**. 728-735.
- Box G.E. and Hunter J.S. (1954). A confidence region for the solution of a set of simultaneous equations with an application for exploration design. *Biometrika*. **41**(1/2), 190-199.
- Bradford, C.J.M. and Vannice, A.M. (1999). CO₂ reforming of CH₄ over supported Ru catalyst, *Journ. of Catal.*, **183**, 69-78
- Bridgewater A. (2008). Progress in Thermochemical Biomass Conversion. Wiley Publishers and John Wiley & Sons. Oxford, Malden. 246.
- Brooks, K.P, Hu, J., Zhu, H, and Kee, R.J (2007). Methanation of Carbon Dioxide by Hydrogen Reduction using the Sabastier Process in Microchannel Reactors. *Chemical Engineering Science*. **62**. 1161-1170.
- Buang N.A. Wan Abu Bakar W.A. Marsin F.A. and Razali M.H. (2008). CO₂/H₂ methanation on nickel oxide based catalysts doped with various elements for the purification of natural gas. *The Malaysian Journal of Analytical Sciences*. **12**(1). 217-223.
- Carpentier P. Royant A. Ohana J. Bourgeois D. (2007). Advances in spectroscopic methods for biological crystals. Part 2: Raman Spectroscopy. *J. Appl. Crystallogr.* **40**. 1113-1122.

- Chakradhar P.S. Murali A. Rao J.L. (2000). A study of electron paramagnetic resonance and optical absorption in calcium manganese phosphate glasses containing praseodymium. *Journal of materials science*. **35**. 353-359.
- Chen L.B. Yin X.M. Mei L. Li C.C. Lei D.N. Zhang M. Li Q.H. Xu Z. Xu C.M. and Wang T.H. (2012). Mesoporous SnO₂ @ carbon core-shell nanostructures with superior electrochemical performance for lithium ion batteries. *Nanotechnology*. **23**(3).1-6.
- Chen, X. Zhou, H. Chen, S. Dong, X. and Lin, W. (2007). Selective oxidation of CO in excess H₂ over Ru/Al₂O₃ catalyst modified with metal oxide. *Journal of Natural Gas Chemistry*, **16**, 409-414.
- Chenakin S.P. Melaet G. Szukiewicz R. Kruse N. (2014). XPS study of the surface chemical state of a Pd/(SiO₂ + TiO₂) catalyst after methane oxidation and SO₂ treatment. *Journal of Catalysis*. **312**. 1-11.
- Choe S.J. Kang H.J. Kim S.J. Park S.B. Park D.H. and Huh D.S. (2005). Adsorbed carbon formation and carbon hydrogenation for CO₂ methanation on the Ni(III) surface- ASED-MO study. *Bull Korean Chem Soc*. **26**(11). 1682-1688.
- Choi C. S. and Jun J. H. (1998). The Influence of Mn Content on Microstructure and Damping Capacity in Fe- (17-23)% Mn Alloys. *Material Science and Engineering: A* **1** (252). 133-138.
- Christoes L. Annaliese E.T. Kylie J.M. Khalil A.A. and George C. (2014). Manganese/cerium clusters spanning a range of oxidation levels and CeMn₈, Ce₂Mn₄, and Ce₆Mn₄ Nuclearities: structural, magnetic, and EPR properties. *Inorganic Chemistry*. **53**. 6805-6816.
- Chun T. P., Hsing K. L., Biing J. L. and Yin Z. C. (2011). Removal of CO in Excess Hydrogen over CuO/Ce_{1-x}Mn_xO₂ Catalyst. *Chemical Engineering Journal* **172**.452-458.
- Chunhui Z. Yifeng Z. Huazhang L. (2010). Effect of samarium on methanation resistance of activated carbon supported ruthenium catalyst for ammonia synthesis. *Journal of Rare Earths*. **28**. 552-555.
- Chung J. Park J.H. Park J.G. Choi B.H. Oh S.J. Cho E.J. Kim H.D. Kwon Y.S. (2001). Photoemission study of rare earth ditelluride compounds (ReTe₂: Re = La, Pr, Sm, and Gd). *Journal of the Korean Physical Society*. **38**(6). 744-749.

- Coates J.P. (1998). 'A review of sampling methods for infrared spectroscopy' in *Applied Spectroscopy: a compact reference for practitioners* eds. J. Workman, A.W. Sprinsteen, Academic Press, New York. 49-91.
- Contreras, J.L., Fuentes, G.A., Zeifert, B., Salmones, J. (2009), Stabilization of supported platinum nanoparticles on γ -alumina catalysts by addition of tungsten, *Journal of Alloys and Compounds*, **483**(1-2), 371-373.
- Cornell J.A. (1990). *How to Apply Response Surface Methodology*. The ASQC Basic References in Quality Control: Statistical Techniques, Vol.8, ASQC, Wisconsin
- Cox P.A. (1995). *The element on Earth-Inorganic Chemistry in the Environment*. Oxford. Oxford University Press. 147-158.
- Curry, R. N. (1981). *Fundamental of Natural Gas Conditioning*. Oklahoma: Penwell Books Publishing Company. pp 66-67.
- Djebaili K. Mekhalif Z. Boumaza A. and Djelloul. (2015). XPS, FTIR, EDX, and XRD analysis of Al_2O_3 scales grown on PM2000 alloy. *Journal of Spectroscopy*. 1-16.
- Djinovic P. Galletti C. Specchia S. Specchia V. (2011). CO methanation over Ru- Al_2O_3 catalysts: effect of chloride doping in reaction activity and selectivity. *Top Catal.* **54**. 1042-1053.
- Dortmundt, D. and Doshi, K. (1999). *Recent Development in CO_2 Removal Membrane Technology*. UOP LLC, Des Plaines, Illinois. USA.1-31
- Dow W.P. Wang Y.P. and Huang T.J. (2000). TPR and XRD studies of yttria-doped ceria/ γ -alumina supported copper oxide catalyst. *Applied Catalysis A:General.* **190**: 25-34.
- Du, G., Lim, S., Yang, Y., Wang, C., Pfefferle, L. and Haller, G.L. (2007). Methanation of carbon dioxide on Ni-incorporated MCM-41 catalysts: The influence of catalyst pretreatment and study of steady state reaction. *Journal of Catalysis.* **249**. 370-379.
- Duhan S. and Aghamkar P. (2008). Influence of temperature and time on Nd_2O_3 - SiO_2 composite prepared by the sol-gel process. *Acta Physica Polonica A.* **113**(6). 1671-1672.
- Durgasari D.N. Vinodkumar T. Sudarsanam P. Raddy B.M. (2014). Nanosized CeO_2 - Gd_2O_3 mixed oxides: Study of structural characterization and catalytic CO oxidation activity. *Catt Lett.* **144**. 971-979.

- Elise B.F. Adam F.L. Karen W. Chunshai S. (2008). In-situ XPS study on the reducibility of Pd-promoted Cu/CeO₂ catalysts for the oxygen-assisted water gas shift reaction. *Top Catal.* **49**. 89-96.
- Ertesva, I.S., Kvamsdal, H. M. and Bolland, O. (2005). Energy Analysis of Gas Turbine Combined-Cycle Power Plant with Pre-combustion CO₂ Capture. *Energy*. **30**, 5-39.
- Falconer J.L and Zagli A.E. (1980). Adsorption and methanation of carbon dioxide on a nickel/silica catalyst. *J.Catalysis*. **62**. 280-285.
- Fierro J.L.G. and Oliván A.M. (1985). Catalytic implication of the unstable lattice oxygen of praseodymium oxide. *Journal of the Less-Common Metals*. **107**. 331-343.
- Finch, J.N. and Ripley, D.L. (1976). United States Patent 3988334. Retrieved on October 26, 1976 from <http://www.freepatentsonline.com/>
- Finger L. W., Cox O. E. and Jephcoat A. P. (1994). A Correction for Powder Diffraction Peak Symmetry due to Axial Divergence. *Journal of Applied Cryst* **27** (6). 892-900
- Fisher I.A. and Bell A.T. (1996). A comparative study of Co and CO₂ hydrogenation over Rh/SiO₂. *J. Catal.* **162**. 54-65.
- Fujita, S., Terunuma, H., Nakamura, M. and Takezawa, N. (1991). Mechanisms of Methanation of CO and CO₂ over Ni. *Industrial & Engineering Chemistry Research*. **30**(6): 1146–1151.
- Furimsky, E., Massoth, F. E. (1993). Introduction of regeneration of hydroprocessing catalysts. *Catalysis Today*. **17** (4): 537-659.
- Gabor A. S. and Yimin L. (2010). Major success of theory and experiment-combined studies in surface chemistry and heterogeneous catalysis. *Top Catal.* **53**. 311-325.
- Galuszka J. Chang J.R. and Amenomiya Y. (1981). Investigation of surface species in methanation of carbon monoxide on a supported nickel catalyst. *Stud. Surf. Sci. Catal.* **7A**. 529-541.
- Gandia L.M. Vicenta M.A. and Gil A. (2000). Preparation and characterization of manganese oxide catalysts supported on alumina and zirconia-pillared clays. *Applied Catalysis A:General*. **196**. 281-292.

- Garcia A.P. Ramos E.R. Angel G.D. Navarrete J. and Contreas C.A. (2007). Catalytic activity of supported cobalt catalyst in the crotonaldehyde hydrogenation reaction. *The AzoJournal of Materials Online*. 3.
- Gardner, D.C. and Bartholomew, C.H. (1981). Kinetics of carbon deposition during methanation of CO. *Industrial and Engineering Chemistry Product Research and Development*. **20** (1), 80-87.
- Gil A. Gandia L.M. Korili S.A. (2004). Effect of the temperature of calcination on the catalytic performance of manganese and samarium-manganese based oxides in the complete oxidation of acetone. *Applied Catalysis A:General*. **274**. 229-235.
- Gong L. Luo L.T. Wang R. Zhang W. (2012). Effect of preparation methods of CeO₂-MnO_x mixed oxides on preferential oxidation of CO in H₂-rich gases over CuO-based catalysts. *J. Chil. Chem.Soc.* **57**. 1048-1053.
- Gorke, O.; Pfeifer, P. & Schubert, K. (2005). Highly selective methanation by the use of a microchannel reactor. *Catalysis Today*, **110**, 132-139.
- Gupta A. Waghmare U.V. Hegde M.S. (2010). Correlation of oxygen storage capacity and structural distortion in Transition metal, Noble metal, and Rare earth ion substituted CeO₂ from first principles calculation. *Chem Mater*. **22**. 5184-5198.
- Gupta, N. M., Kamble, V. S., Iyer, R. M., Thampi, K. R. and Gratzel, M. (1993). FTIR studies on the CO, CO₂ and H₂ co-adsorption over Ru-RuO_x/TiO₂ catalyst. *Catalysis Letters*. **21**: 245–255.
- Habazaki, H., Yamasaki, M., Zhang, B., Kawashima, A., Kohno, S., Takai, T. and Hashimoto, K. (1998). Co-Methanation of Carbon Monoxide and Carbon Dioxide on Supported Nickel and Cobalt Catalysts Prepared from Amorphous Alloy. *Applied Catalysis A: General*. **172**: 131-140.
- Haldor Topsøe A/S,(2005), Methanation of CO over Nickel Mechanism and Kinetics at High H₂/Co ratios. *J Phys Chem B*. **109**(6):2432-8
- Hansheng L. Hang X. Jinfu W. (2011). Methane reforming with CO₂ to syngas over CeO₂-promoted Ni/Al₂O₃-ZrO₂ catalysts prepared via a direct sol-gel process. *Journal of Natural Gas Chemistry*. **20**(1). 1-8.
- He H.Q. Zhang L. Wu H. Li C.Z. Jig S.P. (2011). Synthesis and characterization of doped La₉ASi₆₀26.5 (A= Ca,Sr,Ba) oxy apatite electrolyte by water-based gel-casting route. *International Journal of Hydrogen Energy*. **36**(11). 6862-6874.

- Henni, S. and Herman, K.W. (1991). Method for the regeneration of spent alumina-based catalysts. European Patent 0244014B1. Retrieved on August 21, 1991.
<http://www.yellowpages.com.my/energyguide/>
- Herden N. (2008). Surface Chemistry of Molybdena containing catalysts. Thesis of the doctoral (PhD). Institutional department of environmental engineering and chemical technology. Faculty of Engineering, University of Pannonia. Veszprem. 56-80.
- Herranz, T., Rojas, S., Perez-Alonso, F.J., Ojeda, M., Terreros, P. And Fierro, J.L.G. (2006). Hydrogenation of carbon oxides over promoted Fe-Mn catalysts prepared by the microemulsion methodology. *Applied Catalysis A: General*. **311**(1-2), 66-75.
- Holden N.E. and Coplen T. (2004). The periodic Table of the elements (IUPAC). **26**(1).8.
- Holgado J.P. Alvarez R. and Munvera G. (2000). Study of CeO₂, XPS spectra by factor analysis: Reduction of CeO₂. *Applied Surface Science*. **161**. 301-315.
- Hou, Z and Chen P. (2006). Production of synthesis gas via methane reforming with CO₂ on noble metals and small amount of noble-(Rh-) promoted Ni catalysts. *International Journal of Hydrogen Energy* **31** 5: 555-561.
- Hu, D., Gao, J., Ping, Y., Jia, L., Gunawan, P., Zhong, Z., Xu, G., Gu, F. and Su, F. (2012). Enhanced Investigation of CO Methanation over Ni/Al₂O₃ Catalysts for Synthetic Natural Gas Production. *Industrial & Engineering Chemistry Research*. **51**: 4875-4886.
- Hussain S.T. Naheed R. Badshah A. and Mohmood T. (2009). Design and synthesis of nanoheterogeneous supported catalysts for olefin polymerization. *African Journal of Pure and Applied Chemistry*. **3**(12). 247-261.
- Hyun Y. K., Hyuck M.L, Jung N. P.(2010). Bifunctional Mechanism of CO₂ Methanation on Pd-MgO/SiO₂ Catalyst: Independent Roles of MgO and Pd on CO₂ Methanation. *J.Phys.Chem*. **114**. 7128-7131.
- Inui, T (1996). Highly Effective Conversion of Carbon Dioxide of Available Compounds on Composite Catalyst. *Catalyst Today*. **29**. 329-33.
- Ismail N.S. and Ishak M.B. (2011). Green Technology Policy on Energy in Malaysia. Master of Environment. Universiti Putra Malaysia, Serdang, Selangor.

- James Wills, P.E, Mark S. (2009). Production of Pipeline-Quality Natural Gas with the Molecular Gate CO₂ Removal Process. Guild Associates, Inc
- Jiajian G. Chunmiao J. Jing L. Meiju Z. Fangna G. Guangwen X. Ziyi Z. Fabing S. (2013). Ni/Al₂O₃ catalysts for CO methanation: effect of Al₂O₃ supports calcined at different temperatures. *Journal of Energy Chemistry*. **22**(6). 919-927.
- Jianjun G. Lou H. Zhao H. Chai D. and Zheng X. (2004). Dry reforming of methane over nickel catalyst supported on magnesium aluminate spinels. *Applied Catalysis A: General*. In Press.
- Jinghuan C. Wenbo S. Junhua L. (2011). Catalytic combustion of methane over cerium-doped cobalt chromite catalysts. *Catalysis Today*. **175**(1). 216-222.
- Joglekar, A.M. and May A.T.(1987). Product Excellence through Design of Experiments. *Cereal Foods World*. **32**. 857-868.
- Jones C. Cole K.J. Taylor S.H. Crodace M.J. and Hutchings G.J. (2009). Copper manganese oxide catalysts for ambient temperature carbon monoxide oxidation:effect of calcination on activity. *Journal of Molecular Catalysis A: Chemical*. **305**(1-2). 121-124.
- Kapteijin F. Van Langeveld A.D. Moulijin J.A. Andreini A. Vuurman M.A. Turek A.M. Jehng J.M. and Wachs I.E. (1994). Alumina-supported manganese oxide catalysts. I characterization:effect of precursor and loading. *J. Catal.* **150**. 94-104.
- Karelovic A. and Ruiz P. (2013). Mechanistic study of low temperature CO₂ methanation over Rh/TiO₂ catalysts. *Journal of Catalysis*. **301**. 141-153.
- Ketzial J.S.S.J. Radhika D. and Nesaraj A.S. (2013). Low temperature preparation and physical characterization of doped BaCeO₃ nanoparticles by chemical precipitation. *International Journal of Industrial Chemistry*. **4**(18). 1-13.
- Kijlstra W.S. Poels E.K. and Blick A. (1997). Characterization of Al₂O₃ supported manganese oxide by electron spin resonance and diffuse reflectance spectroscopy. *J Phys Chem B*. **101**. 309-316.
- Kikuchi R. Takada K. Sekizawa K. Sasaki K. Eguchi K. (2001). Thick-film coating of hexaaluminate catalyst on ceramic substrates and its catalyst activity for high temperature methane combustion. *Applied Catalysis A: General*. **218**. 101-111.

- Kim M.Y. Choi J.S. Toops T.J. Jeong E.S. Han S.W. Schwartz V. and Chen J. (2013). Coating SiO₂ support with TiO₂ or ZrO₂ and effects on structure and CO oxidation performance of Pt catalysts. *Catalysts*. **3**(1). 88-103.
- Kim Y.H. Park E.D. Lee H.C. Lee K.H. Kim S. (2007). Natural gas conversion VIII. Proceedings of the 8th Natural Gas Conversion Symposium, May 27-31, Amsterdam, Netherlands. 171.
- Kok E. Scott J. Cant N. Trimm D. (2011). The impact of ruthenium, lanthanum and activation conditions on the methanation activity of alumina supported cobalt catalysts. *Catalysis Today*. **164**(1). 297-301.
- Kozhukharov, V., Machkova, M. and Brashkova, N. (2003). Sol-gel route and characterization of supported perovskites for membrane applications. *Journal of Sol-Gel Science and Technology*. **26**, 753-757.
- Langmuir I. (1915). Chemical reaction at low pressures. *J. Am. Chem. Soc.* **37**(5). 1139-1167.
- Lansink Rotgerink H.G.J. Paalman R.P.A.M. Van Ommen J.G. and Ross J.R.H. (1988). Studies on the promotion of nickel-alumina coprecipitated catalysts. II Lanthanum oxide. *Applied Catalysis*. **45**. 257-280.
- Larachi F. Pierre J. Adnut A. Bermis A. (2002). Ce 3d XPS study of composite Ce_xMn_{1-x}O_{2-y} wet oxidation catalysts. *Applied Surface Science*. **195**. 236-250.
- Lau L.C. Tan K.T. Lee K.T. and Mohamed A.R. (2009). A comparative study on the energy province in Japan and Malaysia in fulfilling their nations, obligations towards the Kyoto Protocol. *Energy Policy*. **37**. 4771-4778.
- Lee S.M. Park K.H. Kim S.S. Kwon D.W. and Hong S.C. (2012). Effect of the Mn oxidation state and lattice oxygen in Mn-based TiO₂ catalysts on the low-temperature selective catalytic reduction of NO by NH₃. *Journal of the Air and Waste Management Association*. **62**(9): 1085-1092.
- Li, C., Sakata, Y., Arai, T., Domen, K. and Maruya, K. (1989). Carbon Monoxide and Carbon Dioxide Adsorption on Cerium Oxide studied by Fourier-transform Infrared Spectroscopy. *Journal of Chemical Society: Faraday Transaction*. **85**(4): 929-943.
- Li T. Yang Y. Zhang C.H. An X. Wan H. Tao Z. Xiang H.W. Li Y.W. Yi F. and Xu B. (2007). Effect of manganese on an iron-based Fischer-Tropsch synthesis catalyst prepared from ferrous sulfate. *Fuel*. **86**(7-8). 921-928.

- Li Y.W. He D. Zhu Z. Zhu Q. Xu B. (2007). Properties of $\text{Sm}_2\text{O}_3\text{-ZrO}_2$ composite oxides and their catalytic performance in isosynthesis. *Applied Catalysis A: General*. **319**. 119-127.
- Liang H.Y. Chen G. Desinan S. Rosei R. Rosei F. and Ma D. (2012). In situ facile synthesis of ruthenium nanocluster catalyst supported on carbon-black for hydrogen generation from the hydrolysis of ammonia-borane. *International Journal of Hydrogen Energy*. **37**. 17921-17927.
- Liang Y.M. Zhang H. Tian Z. Zhu X. Wang X. and Yi B. (2006). Synthesis and structure-Activity relationship exploration of carbon-supported PtRuNi nanocomposite as a Co-tolerant electrocatalyst for proton exchange membrane fuel cells *J Phys Chem B*. **110**. 7828-7834.
- Lin W.W. Cheng H.Y. Ming J. Yu Y.C. Zhao F.Y. (2012). Deactivation of Ni/TiO₂ catalyst in the hydrogenation of nitrobenzene in water and improvement in its stability by coating a layer of hydrophobic carbon. *J. Catal.* **291**. 149-154.
- Liu N. Yan G.Y. Xu S.J. (2005). Phase separation and transport behavior in $\text{La}_{67-x}\text{Sm}_x\text{Sr}_{0.33}\text{MnO}_3$ system. *Chem Res Chinese U*. **21**(6). 706-713.
- Long R.Q. and Wan H.L. (1997). Comparison of praseodymium oxide and SrF₂-promoted praseodymium oxide catalysts for oxidative coupling of methane. *J. Catal.* **172**(2). 471-474.
- Lours P. Alexis J. Bernhart G. (1998). Oxidation resistance of ODS alloy PM2000 from 880°C to 1400°C. *Journal of materials science letters*. **17**. 1089-1093.
- Lowell S. Shield J.E. Thomas M.A. and Thommes M. (2004). Characterization of porous solids and powders: surface area, pore size, and density. Kluwer Academic Publishers, the Netherlands.
- Lu C.S. Chen C.C. Huang L.K. Antsai P. Lai H.F. (2013). Photocatalytic degradation of Acridine Orange over NaBiO₃ driven by visible light irradiation. *Catalysts*. **3**(2). 501-516.
- Luisetto I. Tuti S. and Bartolomeo E.D. (2012). Co, Ni supported on CeO₂ as selective bimetallic catalyst for dry reforming of methane. *International Journal of Hydrogen Energy*. **57**. 15992-15999.
- Luo L. and Li S. (2004). Effect of transition metals on catalytic performance of Ru/Sepolite catalyst for methanation of carbon dioxide. *Journal of natural gas chemistry*. **13**. 45-48.

- Mansouri M. Atashi H. Mohammad M. Khalilipour, Setaresheenas N., and Shahraki F. (2013). Rate expression of Fischer-Tropsch synthesis over Co-Mn nanocatalyst by Response Surface Methodology (RSM). *Journal of the Korean Chemical Society*. **57**(6). 769-777.
- Marc J. Antoine Beuls, Patricio R. (2010). Catalytic production of methane from CO₂ and H₂ at low temperature: Insight on the reaction mechanism. *Catalyst Today*. **157**. 462-466.
- Marie Loren Y Palero, Leonila C. Abella and Teddy G. Monroy. (2012). Optimization of process parameters of methane decomposition in a fluidized bed reactor using Ni-Cu/Al₂O₃ catalysts. *International Journal of Chemical Engineering and Applications*, **3**:157.
- Marwood, M., Doepper, R. and Renken, A. (1997). In-situ surface and gas phase analysis for kinetic studies under transient conditions: The catalytic hydrogenation of CO₂. *Applied Catalysis A: General*. **151**: 223-246.
- Mazzieri V.A. Sad M.R. Veray C.R. Picck C.L. and Grau R. (2010). Preparation and characterization of Ru-Sn/Al₂O₃ catalysts for the hydrogenation of fatty acid methyl esters. *Quim Nova*. **33**(2). 269-272.
- Md. Yassin, A. A. (1987). "Natural-gas future energy for Malaysia." Kuala Lumpur, Malaysia: Simposium Ketige Jurutera Kimia Malaysia.
- Mei Z. Li Y. Fan M. Argyle M.D. and Tang J. (2014). The effect of bimetallic Co-Ru nanoparticles on Co/RuO₂/Al₂O₃ catalysts for the water gas shift and methanation. *International Journal of Hydrogen Energy*. **39**. 14808-14816.
- Meng F. Zhong P. Li Z. Lui X. and Zheng H. (2014). Surface structure and catalytic performance of Ni-Fe catalyst for Low-temperature CO hydrogenation. *Journal of Chemistry*. 1-7.
- Michael K. Golab A. Shulakova V. Ennis-Kinga J. Allinson G. Sharma S. Aiken T. (2010). Geological storage of CO₂ in saline aquifers- A review of the experience from existing storage of operation. *Int. J. Greenh. Gas Control*. **4**. 659-667.
- Michiaki Y., Mtsuru K., Eiji A. Hiroki H., Asahi K., Katsuhiko A., Koji H. (1999). CO₂ methanation catalysts prepared from amorphous Ni-Zr-Sm and Ni-Zr-misch metal alloy precursors. *Jornal material science & engineering*. Institute for materials research, Tohoku University, Sendai, Japan.

- Mills G. A. and Fred W.S. (1974). Catalytic Methanation. *Catalysis Review: Science and Engineering*. **8**(1). 159-210.
- Mina C. Nairmen, Manzanares I. Caballero, Julio F. (1996). Molecular constants of carbon monoxide at $v= 0,1,2$ and 3. *Journal of Chemical Education*. **73**(8) 804-807.
- Mohajeri, S. Aziz, H.A. Isa, M.H. Zahed, M.A. Adlan, M.N. (2010). Statistical Optimization of Process Parameters for Landfill Leachate Treatment using Electro-Fenton Technique. *J. Hazard. Mater.* **176**. 749-758.
- Mohamed A.R. (2003). The Development of Manganese Oxide Based Catalyst Materials Ageing for Emission Control: Synthesis, Catalytic Activity and Characterization. M.Sc. Thesis. Universiti Teknologi Malaysia, Skudai
- Montgomery. D.C. (1997). Design and Analysis of Experiments. 4th Ed. Wiley. New York.
- Montgomery D.C. (1999). Experimental design for product and process design and development. *The Statistician*. **48**(2). 159-177.
- Mori, S., Xu, W. C., Ishidzuku, T., Ogasawara, N., Imal, J and Kobayashi, K. (1998). Mechanochemical Activation of Catalysts for CO₂ Methanation. *Applied Catalysts A: General*. **137**. 225-269
- Munnik P. Velthoen M.E. De Jongh P.E. De jong K.P. Gommers C.J. (2014). Nanoparticle growth in supported nickel catalysts during methanation reaction-larger is better. *Angew-Chem. Int. Ed. Engl.* **53**(36). 1493-1497.
- Murata, K., Okabe, K., Inaba, M., Takahara, I. and Liu., Y. (2009). Mn-modified Ru catalysts supported on carbon nanotubes for Fisher Tropsch synthesis. *Journal of the Japan Petroleum Institute* **52**(1), 16-20.
- Myers R.H. Khuri A.I. and Vining G. (1992). Response surface alternative to the Taguchi robust parameter design approach. *The American Statistician*. **46**(2). 131-139.
- Narain K. Yazdani T. Bhat M.M. and Yunus M. (2012). Effect on physico-chemical and structural properties of soil emended with distillery effluent and ameliorated by cropping two cereal plant spp. *Environ Earth Sci.* **66**. 977-984.
- Navarro R.M. Pena M.A. and Fierro J.L.G. (2007). Hydrogen production reactions for carbon feedstocks:Fossil fuels and biomass. *Chem. Rev.* **107**. 3952-3991.

- Nefedov, V.I., Gati, D., Dzhurinskii, B.F., Sergushin, N.P. and Salyn, Ya.V. (1975). Simple and coordination compounds. *Russian Journal of Inorganic Chemistry*. **20**, 2307-2314.
- Nguefack M. Popa A. Rossignols, Kappenstein C. (2003). Preparation of alumina through a sol-gel process- synthesis, characterization, thermal evolution and model of intermediate boelmite. *Physical Chemistry Chemical Physics*. **5**(19). 4279-4289.
- Nguyen T.D. Mrabet O. and Do T.O. (2008). Controlled self-assembly of Sm_2O_3 nanoparticles into nanorods: Simple and large scale synthesis using bulk Sm_2O_3 powders. *J.Phys.Chem C*. **112**. 15226-15235.
- Nguyen T.D. Dinh C.T. and Do T.O. (2009). Monodisperse samarium and cerium orthovanadate nanocrystals and metal oxidation states on the nanocrystals surface. *Langmuir*. **25**(18). 11142-11148.
- Niemant J.W. (2007). Spectroscopy in catalysis. Wiley-VCH Weinheim.
- Nurunnabi, M., Murata, K., Okabe, K., Inaba, M. and Takahara, I. (2008). Performance and Characterization of $\text{Ru}/\text{Al}_2\text{O}_3$ and Ru/SiO_2 Catalysts Modified with Mn for Fischer–Tropsch Synthesis. *Applied Catalysis A:General*. **340**, 203-211.
- Osman A.E.M. Lott K.A.K. Hogarath C.A. Hassan M.A. (1988). A study of electron spin resonance in copper-phosphate glasses containing praseodymium. *Journal of Material Science*. **23**. 1098-1101.
- Pan T.M. and Yu T.Y. (2009). Comparison of the structural properties and electrical characteristics of Pr_2O_3 , Nd_2O_3 and Er_2O_3 charge trapping layer memories. *Semicond. Sci. Technol*. **24**(9). 1-8.
- Panagiotopolou, P. & Kondarides, D.I. (2007). A comparative study of the water-gas shift activity of Pt catalysts supported on single (MO_x) and composite ($\text{MO}_x/\text{Al}_2\text{O}_3$, MO_x/TiO_2) metal oxide carriers. *Catalysis Today*. **127**. 319-329
- Panagiotopoulou, P., Dimitris I. Kondarides and Xenophon E. Verykios. (2008). Selective Methanation of CO over Supported Noble Metal Catalysts: Effects of the Nature of the Metallic Phase on Catalytic Performance. *Applied Catalysis A: General*. **344**, 45-54.

- Panagiotopoulou, P., Kondarides, D.I. and Verykios, X.E. (2009). Selective methanation of CO over supported Ru catalysts. *Appl Catal B: Environmental*. **88**, (3-4): 470-478
- Pandey D and Deo G. (2015). Determining the best composition of a Ni-Fe/Al₂O₃ catalyst used for the CO₂ hydrogenation reaction by applying response surface methodology. *Chemical Engineering Communication*. In Press.
- Parthasarathi B.M. Rajamathi M.S. Hedge and Kamath P.R. (2000). Thermal behavior of hydroxides, hydroxysalt and hydrotalcites. *Bull Mater Sci*. **23**(2). 141-145.
- Park, S.E.; Nam, S.S.; Choi, M.J. & Lee, K.W. (1995). Catalytic Reduction of CO₂: The Effects of Catalysts and Reductants. *Energy Conversion Management*, **26**, 6-9.
- Parpinello G.P. and Versari A. (2000). A simple high-performance Liquid Chromatography method for the analysis of glucose, glycerol and methanol in a bioprocess. *Journal of Chromatographic Science*. **38**. 259-261.
- Peluso M.A. Hernandez W.Y. Dominguez M.I. Thomas H.J. Centeno M.A. and Sambeth J.E. (2012). CO oxidation: Effect of Ce and Au addition on MnOx catalysts. *Latin American Applied Research*. **42**. 351-358.
- Perego, C. and Villa, P. (1997). Catalyst preparation methods. *Catalysis Today*. **34** (3-4), 281-305.
- Perkas N. Amirian G. Zhong Z. Teo J. Gofer Y. and Gedanken A. (2009). Methanation of carbon dioxide on Ni catalysts on mesoporous ZrO₂ doped with rare earth Oxides. *Catal Lett*. **130**. 455-462.
- Phan T.L. Zhang P. Tran H.D. and Yu S.C. (2010). Electron spin resonance study of Mn-doped metal oxides annealed at different temperatures. *Journal of the Korean Physical Society*. **57**(5). 1270-1276.
- Piyapong H. Phavaneo N. Sabaithip T.K. Karn P.S. Nuwong C. Hussanai S. and Prayut J. (2013). A comprehensive small and pilot scale fixed bed reactor approach for testing Fischer-Tropsch catalyst activity and performance on a BTL route. *Arabian Journal of Chemistry*. In press.
- Pojanavaraphan C. Luengnarue mitchal A. Gulari E. (2013). Catalytic activity of Au-Cu/CeO₂-ZrO₂ catalysts in steam reforming of methanol. *Applied Catalysis A: General*. **456**. 135-143.

- Ponee V. (1978). Some aspects of the mechanism of methanation and Fischer-Tropsch Synthesis. *Catalysis Review: Science and Engineering*. **18**(1). 151-171.
- Praire M.R. Renken A. Highfield J.G. Ravindranathan K. Gratzel M. (1991). Fourier Transform Infrared Spectroscopic Study of CO₂ Methanation on Supported Ruthenium. *J. Catal.* **129**. 130-144.
- Profeti, L.P.R., Ticianelli, E.A. and Assaf, E.M. (2008). Co/Al₂O₃ catalysts promoted with noble metals for production of hydrogen by methane steam reforming. *Fuel*. **87**, 2076 -2081.
- Puduki M. and Yaakob Z. (2014). Catalytic aspects of ceria zirconia solid solution: Part II An overview on recent developments in the heterogenous catalytic application of metal loaded ceria-zirconia solid solution. *Der Pharma Chemica*. **6**(1). 224-240.
- Radler, M. Worldwide Look at Reserves and Production. *Oil & Gas Journal*. (2003). **49**. 46-47.
- Radu C. (1998). Structure/Activity Correlation for Unpromoted and CeO₂-promoted MnO₂/SiO₂ Catalyst. *Catalysis Letters* **55**. 25-31
- Rahman S. Rezaei M. Meshkani F. (2013). Ni/Al₂O₃ nanocatalyst for CO₂ methanation. International Biennial Conference on Ultrafine Grained and Nanostructured Materials. 5-6 November 2013. Tehran, Iran.
- Razak M.R.A. and Ramli M.R. (2008). A brief presentation on the Malaysia electricity supply industry. Bangkok, Thailand. Conference Fuel options for Power Generation.
- Razali M.H. Wan Abu Bakar W.A. Buang N.A. Marsin F.M. (2005). CO₂/H₂ methanation on nickel oxide based catalysts doped with lanthanide series. *Malaysian Journal of Analytical Sciences*. **9**(3). 492-496.
- Raupach M.R. Marland G. Clais P. Quare C.L. Canadell J.G. Klepper G. and Field C.B. (2007). Global and regional drivers of accelerating CO₂ emission: *Proceeding of the National Academy of Sciences of the United States of America*. **104**(24). 10288-10293.
- Rostrup-Nielsen J.R. Pedersen K. Sehested J. (2007). High temperature methanation sintering and structure sensitivity. *Applied Catalysis A: General*. **330**. 134-138.

- Russel W.W. and Miller G.H. (1950). Catalytic hydrogenation of carbon dioxide to higher hydrocarbons. *J. Am. Chem. Soc.* **72**. 2446.
- Rynkowski J. Farbotko J. Touroude R. and Hilaire L. (2000). Redox behavior of ceria titania mixed oxide. *Appl.Catal. A:General.* **203**. 335-348.
- Saad M.W.A. (2013). Optimization of carbon dioxide methanation over nickel waded mesoporous silica nanoparticles using response surface methodology. Thesis. Faculty of Chemical Engineering. Universiti Teknologi Malaysia.
- Sabestier P and Senderens J.B. (1902). New synthesis of methane. *Compt. Rend.* **134**. 514-516.
- Salagre, P., Fierro, J.L.G., Medina, F. and Sueiras, J.E. (1996). Characterization of nickel species on several γ -alumina supported nickel samples. *Journal of Molecular Catalysis A: Chemical.* **106**, 125-134.
- Saluko, A. E. (2005). Removal of Carbon Dioxide from Natural Gas for LNG Production. Institute of Petroleum Technology Norwegian University of Science and Technology.
- Savva P. Goundani K. Vakros J. Bourikas K. Founzoula C. Vattis D. Lycourghiotis A. Kordulis C. (2008). Benzene hydrogenation over Ni/Al₂O₃ catalyst prepared by conventional and sol-gel techniques. *Applied Catalysis B: Environmental.* **79**(3). 199-207.
- Schmitz P.J. Usmen R.K. Poters C.R. Graham G.W. and Mc Case R.W. (1993). Effect of calcination temperature on Al₂O₃-supported CeO₂:Complementary from XRD and XPS. *Applied Surface Science.* **72**. 181-187.
- Sehested J. (2003). Sintering of steam reforming catalysts. *Journal of Catalysis.* **217**(2). 417-426.
- Schaper H. Doesburg E.B.M. and Van Reijen L.L. (1985). Thermal stabilization of high surface area alumina. *Appl Catal.* **14**. 371.
- Shamshi H.M. Shaheer A.M. Shim K.B. and Yang O.B. (2010). Morphological and electrochemical properties of crystalline praseodymium oxide nanorods. *Nanoscale Res Lett.* **5**(4). 735-740.
- Sharma, S., Hu, Z., Zhang, P., McFarland, E. W. and Metiu, H. (2011). CO₂ methanation on Ru-doped ceria. *Journal of Catalysis.* **278**: 297-309.
- Silva C.L.S. Marchetti S.G. Farojunior A.C. Silva T.F. Assaf J.M. Rangel M.C. (2012). Effect of gadolinium on the catalytic properties of Iron oxide for WGS. *Catalysis Today.* **213**. 127-134.

- Sittichai N. (2005). M.S. Investigation of Active sites and Reaction Network in Catalytic Hydrogen Production: Steam Reforming of Lower Alkanes and The Water Gas-Shift Reaction. The Ohio State Universit. pp 60-67
- Solymosi, F., Erdehelyi, A. and Bansagi, T. (1981). Methanation of CO₂ on supported rhodium catalyst. *Journal of Catalysis*. **68**: 371-382.
- Song H., Yang J., Zhao J., Chou L. (2010). Methanation of carbon dioxide over a highly dispersed Ni/La₂O₃ catalyst. *Chin J catal*. **31**. 21-33.
- Speight, J.G. (2007). *Natural Gas: A Basic Handbook*. Hounston, Texas: Gulf Publishing Company
- Steppan, D.D Werner, J. Yeater R.P (1998). Essential Regression and Experimental Design for Chemists and Engineers. (1998) [http://geocities.com/siheonvallev.network/1032/CG page.html](http://geocities.com/siheonvallev.network/1032/CG_page.html).
- Stevens, R. W., Siriwardane, R. V and Logan, J. (2008). In Situ Fourier Transform Infrared (FTIR) Investigation of CO₂ Adsorption onto Zeolite Materials. *Energy & Fuels*. **22**(12): 3070–3079.
- Strakey, J. P Forney, A. J. Haynes W.P. (1975). Department of Commerce National Technical Information Service. Energy Research and Development Administration, Pittsburgh, PA. Pittsburgh Energy Centre.
- Stookey, D.J., C.J. Patton, and G.L. Malcolm, "Membranes Separate Gases Selectively," CEP, Nov. 1986, pp. 36–40.
- Stoop, F., Verbiest, A. M. G. and Van Der Wiele, K. (1986). The influence of the support on the catalytic properties of Ru catalysts in the CO hydrogenation. *Applied Catalysis*. **25**: 51-57.
- Su P. Chu O. Wang L. (2010). Studies on catalytic activity of nanostructure Mn₂O₃ prepared by solvent-thermal method on degrading crystal violet. *Modern Applied Science*. **4**(5). 125-129.
- Su, B.L. & Guo, S.D. (1999). Effects of rare earth oxides on stability of Ni/ α -Al₂O₃ catalysts for steam reforming of methane. *Studies in Surface Science and Catalysis*, **126**, 325-332.
- Sudhanshu S. Zhenpeng H. Peng Z. Eric W.M. and Itoria M. (2011). CO₂ methanation on Ru-doped Ceria. *J. Catal*. **278**. 297-309.
- Suzuki C. Kawai J. Takahashi M. Vlaicu A.M. Adachi H. Mukoyama T. (2000). The electronic structure of rare earth oxides in the creation of the core hole. *Chemical physics* **253**. 27-40.

- Szailer, E.N., Albert, O. and Andra, E. (2007). Effect of H₂S on the hydrogenation of carbon dioxide over supported Rh Catalysts. *Topics in Catalysis*.46.
- Teramura K. Tanaka T. Ishikawa H. Kohno Y. and Fiunaka T. (2004). Photocatalytic reduction of CO₂ to CO in the presence of H₂ or CH₄ as a reductant over MgO. *J Phys Chem B*. **108**. 346-356.
- Takenaka, S., Shimizu, T. and Otsuka, K. (2004). Complete removal of carbon dioxide in hydrogen-rich gas stream through methanation over supported metal catalysts. *International Journal of Hydrogen Energy*. **29**, 1065-1073.
- Takeshi,K. And Aika, K. (1995). Comparison of Carbon Dioxide and Carbon Monoxide with Respect to Hydrogenation on Roney Ruthenium. *Applied Catalyst A.:General*. **133**. 31-45
- Trimm, D.L. (1980). Design of Industrial Catalysts.Vol. 11. Netherlands, USA: Elsevier Science Publisher.
- Toemen S. Wan Abu Bakar W.A. and Ali R. (2014). Investigation of Ru/Mn/Ce/Al₂O₃ catalyst for carbon dioxide methanation: Catalytic optimization, physicochemical studies and RSM. *Journal of the Taiwan Institute of Chemical Engineers*. **45**(5). 2370-2378.
- Truffault L. Ta, M.T. Devers T. Konstantinor K. Harel V. Simmonard C. Andrezza C. Neurkoveti L.P. Pinear A. and Verun D. (2010). Application of nanostructured Ca doped CeO₂ for ultraviolet filtration. *Materials research Bulletin*. **45**. 527-535.
- Vannice, M.A. (1987). The Catalytic Synthesis of Hydrocarbon from H₂/CO Mixtures over the Group VIII Metals. I. The Specific Activities and Product Distributions of Supported Metals. *Journal of Catalyst*. **37**. 449-457.
- Van Rossum, G. J. (1986). *Gas Quality*. Netherland, USA: Elsevier Science Publisher.
- Van Wieringen J.S. (1955). Paramagnetic resonance of divalent manganese incorporated in various lattices. *Discussion Faraday Soc*. **19**. 118.
- Wachs, I.E. (2005). Recent Conceptual Advances in the Catalysis Science of Mixed Metal Oxide Catalytic Materials. *Catalysis Today*. **100**, 79-94.
- Wan Abu Bakar, W.A. Ali, R. Sulaiman, N. and Abdul Rahim, H.F.(2010). Manganese oxide doped noble metals supported catalyst for carbon dioxide methanation reaction. *Transactions C: Chemistry and Chemical Engineering, Scientia Iranica*, **17**, 115-123.

- Wan Abu Bakar, W.A. Othman, M.Y. Ali, R. Ching K.Y. and Toemen, S. (2009). The investigation of active sites on ickel oxide based catalysts towards the in-situ reactions of methanation and desulfurization. *Modern Applied Science*, **2**(3), 35-43.
- Wang, A and Lu, G.Q.(1998). Reforming of Methane with Carbon Dioxide over Ni/Al₂O₃ Catalyst:Effect of Nickel Precursor. *Applied Catalyst A: General*. **169**.271-280
- Wang, S.G., Liao, X.Y., Cao, D.B., Huo, C.F., Li, Y.W., Wang, J.G. & Jiao, H.J. (2007). Factors controlling the interaction of CO₂ with transition metal surfaces. *Journal of Physical Chemistry C*, **111**, 16934-16940.
- Wang W. Wang S.P. Ma X.B. and Gong J.L. (2011). Recent advances in catalytic hydrogenation of carbon dioxide. *Chem Soc. Rev.* **40**. 3703-3727.
- Wang Z. Li X. Song W. Chen J. Li T. Feng Z.P. (2011). Synergetic promotional effects between cerium oxide and manganese oxides for NH₃ selective catalyst reduction over Ce-Mn/TiO₂. *Materials Express*. **1**(2). 167-175.
- Wang Z. Wang Q. Liao Y. Shen G. Gong X. Han N. Liu H. Chen Y. (2011). Comparative study of CeO₂ and doped CeO₂ withtailored system vacancies for CO oxidation. *Chem Phys Chem*. **12**(15). 2763.
- Weatherbee, G.D. and Bartholomew, C.H. (1984). Hydrogenation of CO₂ on Group VIII metals IV. Specific activities and selectivities of silica-supported Co, Fe, and Ru. *Journal of Catalysis*. **87**, 352-362.
- White G.A. Roszkowski T.R. and Stanbridge D.W. (1974). The RM Process. Am. *Chem. Soc. Div. Fuel. Chem.* **19**(3). 57.
- Wijnja H. Schulthess C.P. (1999). ATR-FTIR and DRIFT spectroscopy of carbonate species at the aged γ -Al₂O₃ water interface. *Spectrochim. Acta A*. **55**(4). 861-872.
- William E.L and David E.R. (2005). "Natural Gas Composition". Gas Technology Institute.
- Wolfframm O. Ratzke M. Kappa M. Montenegro M.J. Dobelli M. Lippert T. Reif J. (2004). Pulsed laser deposition of thin Pr_xO_y films on Si(100). *Materials Science and Engineering B*. **109**. 29.
- Wu, J.C.S. & Chou, H.C. (2009). Bimetallic Rh-Ni/BN catalyst for methane reforming with CO₂. *Chemical Engineering Journal*, **148**, 539-545.

- Xavier, K. O. Sreekala, R. K. Rashid, K. A. Yusuff K. K. M. and Sen, B. (1999). Doping Effects of Cerium Oxide on Ni/Al₂O₃ Catalysts for Methanation. *Catalysis Today*, **49**, 17-21
- Xiang W. and You-chang X (2000). Total Oxidation of Methane over La, Ce and Y Modified Manganese Oxide Catalysts. *Reaction Kinetic. Cataly. Letter* **71** (1). 3-11
- Xu, B, Wei, J, Yu, Y., Li, J., and Zhu, Q. (2003). Size Limit of Support Particles in an Oxide-Supported Metal Catalyst: Nanoparticles Ni/ZrO₂ for Utilization of Natural Gas. *J. Phys. Chem. B*. **107**. 5203-5207.
- Yaccato, K., Carhart, R., Hagemeyer, A., Lesik, A., Strasser, P., Volpe, F. A., Trner, H. Jr., Weinberg, H., Grasselli, K. R and Brooks, C. (2005). Competitive CO and CO₂ Methanation over Supported Noble Metal Catalysts in High Throughput Scanning Mass Spectrometer. *Applied Catalysis A: General*. **296**, 30-48.
- Yan X. Liu Y. hao B. Wang Z. Wang Y. Liu C.J. (2013). Methanation over Ni/SiO₂: effect of the catalyst preparation methodology. *International Journal of Hydrogen Energy*. **38**. 2283-2291.
- Young P.W. and Clark. (1973). Metal support interaction and deactivation in copper-based catalysis. *Chem. Eng. Progress*. 69.
- Yusof N. B. M., Mohamad F.I, Ruslan H. (2010). Estimation of Dispersion of Carbon Monoxide (CO), Nitrogen Dioxide (NO₂), and Carbon Dioxide (CO₂) from Port Klang - KLIA Road. Universiti Teknologi Nasional, Malaysia
- Zafiris G.S. and Gorte R.J. (1993). Evidence for a second CO oxidation mechanism on Rh/ceria. *J. Catal.* **139**. 561.
- Zamani A.H. Ali R. Wan Abu Bakar W.A. (2014). The investigation of Ru/Mn/Cu-Al₂O₃ oxide catalysts for CO₂/H₂ methanation in natural gas. *Journal of the Taiwan Institute of Chemical Engineerings*. **45**(1). 143-152.
- Zhang L. Lin J. Ni J. Wong D. Wei K. (2011). Highly efficient Ru/Sm₂O₃-CeO₂ catalyst for ammonia synthesis. *Catalysis Communications*. **15**. 23-26.
- Zhang W.T. Quan S.Q. Xie W.F. and Huang D. (2012). The preparation and characterization of N-F-Sm-TiO₂ sol and its photocatalytic performance for 4-chlorophenol degradation. Proceeding of 2012 international conference on mechanical engineering and materials science. Atlantic Press. 539-542.

- Zhang Y.F. Zhang G. Wang L. Xu Y. Sun Y. (2012). Selective methanation of carbon monoxide over Ru based catalysts in H₂-rich gases. *Journal of Industrial and Engineering Chemistry*. **18**. 1590-1597.
- Zhao A. Ying W. Zhang H. Hongfang M. and Fang D. (2012). Ni/Al₂O₃ catalysts for syngas methanation: effect of Mn promoter. *Journal of Natural Gas Chemistry*. **2**. 170-177.
- Zhao T. Toyama M. Kita K. Kyuno K. Toriumi A. (2006). Moisture-absorption-induced permittivity deterioration and surface roughness enhancement of lanthanum oxide films on silicon. *Appl Phys. Lett.* **88**. 560.
- Zheng, H.Y., An, M.Z. and Lu, J.F. (2008). Surface characterization of the Zn-Al-Al₂O₃ nanocomposite coating fabricated under ultrasound condition. *Applied Surface Science*. **254**, 1644-1650.
- Zhuang, Q., Qin, Y. Chang, L. (1991). Promoting effect of cerium oxide in supported nickel catalyst for hydrocarbon steam-reforming. *Applied Catalyst*. **70**(1): 1-8.
- Zielinska B. Mijowska E. and Kalenczuk R.J. (2012). Synthesis and characterization of K-Ta mixed oxides for hydrogen generation in photocatalysis. *International Journal of Photoenergy*. 1-7.
- Zou, G.P., Cheranghi, N. and Taheri, F. (2005). Fluid-Induced Vibration of Composite Natural Gas Pipelines. *International Journal of Solids and Structures*. **42**. 1253-1268.